IMMUNOTHERAPEUTIC EFFECT OF AN INTERLEUKIN-2 IMMUNOCONJUGATE IN ANIMAL MODEL

LEUNG KIN LUEN

M. PHIL.

THE HONG KONG POLYTECHNIC UNIVERSITY

2003

Acknowledgements

I would like to take this opportunity to thank people who had been very supportive and helpful throughout the entire research study. The most important of all is my supervisor, Dr. Cheuk-Sang Kwok, Associate Professor, Department of Optometry and Radiography. He gave me a lot of valuable guidance and suggestions throughout the study. In addition, I would also like to thank Dr. Timothy Yip, Florence So, Victor Ma of the Radiobiology Lab, Queen Elizabeth Hospital, Hong Kong for their technical assistance in supporting the study. Last but not least, I thank Dr. Wai-Hon Lau, COS of Clinical Oncology, Queen Elizabeth Hospital, for allowing me to carry out most of the research work reported here at the Radiobiology Lab.

Abstract of thesis entitled "Immunotherapeutic Effect of an Interleukin-2 Immunoconjugate in Animal Model" submitted by Leung Kin Luen for the degree of Master of Philosophy at The Hong Kong Polytechnic University in August of 2003.

ABSTRACT

Recombinant antibody-cytokine fusion proteins are immunocytokines that deliver high cytokine concentrations in the targeted tumor microenvironment and thereby effectively stimulate cellular immune responses against human malignancies. Proto-oncogene HER-2/*neu* is overexpressed in some human breast, ovarian, prostate and lung cancers and associated with poor prognosis. A novel immunocytokine consisting of a recombinant human interleukin-2 (rhIL-2) and a recombinant humanized single chain antibody that combined the V_H and V_L portions of a murine monoclonal antibody (520C9) specific for human HER-2/*neu* positive tumors has been developed. The fusion protein H520C9sFv-rhIL-2 in combination with human peripheral blood mononuclear cells effectively inhibited growth and dissemination of subcutaneous xenograft and lung metastases of human HER-2/*neu* positive ovarian carcinoma in severe combined immunodeficient mice. In addition, histological staining and immunohistochemical analysis of lung metastases in the treatment group of SCID mice with the H520C9sFv-rhIL-2 and human PBM cells demonstrated

significant suppression of metastatic tumor growth. A dose dependent response was also demonstrated by the effective inhibition of lung metastases at a dose level of 6 μg H520C9sFv-rhIL-2 instead of 3 μg H520C9sFv-rhIL-2 per injection with 2 x 10^5 human PBM cells. Such results demonstrated that immunocytokine-directed interleukin-2 therapy to tumors sites could be effective in an adjuvant setting for patients with disseminated metastases of human HER-2/*neu* positive tumors.

ABBREVIATIONS

BCIP/NBT: 5-Bromo-4-Chloro-3-Indoxyl Phosphate and Nitro Blue Tetrazolium Chloride

BSA: Bovine Serum Albumin

DMEM: Dulbecco's Modified Eagle's Medium

ELISA: Enzyme Linked Immunosorbent Assay

FITC/AP: Fluorescein IsoThioCyanate / Alkaline Phosphatase

H520C9sFv-rhIL-2: Humanized 520C9sFv / human interleukin-2 fusion protein

IL-1: Interleukin-1

IL-2: Interleukin-2

IL-6: Interleukin-6

INF-γ: Interferon-Gamma

LAK cell: Lymphokine-activated Killer Cell

mAbs: Monoclonal Antibodies

NK cells: Natural Killer Cells

OD: Optical Density

PBS: Phosphate Buffered Saline

PBST: Phosphate Buffered Saline containing 0.05%Tween-20

PBM cells: Peripheral Blood Mononuclear Cells

rhIL-2: Recombinant Human Interleukin-2

SCID: Severe Combined Immunodeficiency Disease

SDS-PAGE: Sodium Dodecyl Sulfate Polyacrylamide Gel Electrophoresis

sFv: Single-chain Fv

TBS: Tris Buffered Saline

TBST: Tris Buffered Saline containing 0.05%Tween-20

TCGF: T Cell Growth Factor

TNF: Tumor Necrosis Factor

V_H: Variable region of heavy chain

V_L: Variable region of light chain

TABLE OF CONTENTS

LIST OF FIGURES

LIST OF TABLES

LIST OF APPENDICES

CHAPTER 1

Introduction

Interleukin-2 (IL-2) is capable of activating and expanding a variety of immune effector cells, including T lymphocytes, natural killer (NK) cells and possibly granulocytes (Whittington and Faulds, 1993). Extensive research demonstrated that high-dose recombinant human interleukin-2 (rhIL-2) therapy has shown success in the treatment of established tumors in both animal models and patients with advanced melanoma or renal cell carcinoma (Dillman 1999, Baars et al 1992, Lotze et al 1986 and Rosenberg et al 1985). However, the clinical use of high-dose rhIL-2 therapy has been limited because of induction of severe systemic toxicities in tissues. In order to overcome dose-limiting side effects, different approaches have been used to target sufficient concentrations of IL-2 to tumor microenvironment.

Monoclonal antibodies (mAbs) have been developed for cancer therapy because they specifically target tumor-associated antigens. By specific binding to such antigens, antibodies can direct an immune response to the tumor. The use of mAbs as a targeting device of

cytotoxic agents seems to be a very attractive approach for the specific elimination of cancer cells, thus overcoming one of the major problems of conventional cancer treatments, such as chemotherapy and radiotherapy, which also damage normal cells to a certain extent. However, major limitations in clinical use of antibodies as delivery agents are their inadequate uptake and poor distribution in tumors, partially due to the large size of the antibodies (Riethmuller et al, 1993).

Recombinant antibody-IL-2 fusion proteins provide an efficient approach for achieving effective local concentrations of IL-2 in the tumor microenvironment to induce local anti-tumor immune responses. Experimental studies indicated that recombinant antibody-IL-2 fusion proteins could induce an immune response capable of eradicating established cancer metastases in animal tumor models (Hornick et al 1999, Melani et al 1998, Xiang et al 1997 and Becker et al 1996).

Research studies reported that the overexpression of HER-2/*neu* proto-oncogene plays a direct role in the pathogenesis and aggressiveness of tumors and is associated with poor clinical outcome

in patients with newly diagnosed primary cancers (Toikkanen et al 1992 and Tandon et al 1989). HER-2/*neu* is an attractive target for active immunotherapy due to its low expression in normal tissues and overexpression in many different types of cancers (Fendly et al, 1990). Recently, a novel antibody-IL-2 fusion protein of a recombinant human IL-2 and a recombinant humanized single chain antibody H520C9sFv has been constructed and characterized to retain both the immunostimulatory effects of IL-2 and specific binding activity against the HER-2/*neu* proto-oncogene (Li et al, 1999). Preliminary experiments to characterize the *in vivo* anti-tumor effect of the fusion protein in a syngeneic mouse tumor model were reported (Kwok et al, 2001). The results demonstrated that the fusion protein, H520C9sFv-rhIL-2, could inhibit the growth of mouse B16 melanoma transfected with human HER-2/*neu* gene. However, the immunotherapeutic effect of the fusion protein in metastatic animal tumors has not yet been tested. It is anticipated that the novel antibody-IL-2 fusion protein would have effective clinical applications in the treatment and/or eradicaton of HER-2/*neu* positive tumors.

1.1 Statement of Purpose

The purpose of this study was to further evaluate the therapeutic potential of the H520C9sFv-rhIL-2 in treating HER-2/*neu* overexpressing tumors in mice. The objectives of the study were to:

1. Develop a human HER-2/*neu* positive metastatic tumor model in SCID mice.

2. Evaluate the anti-tumor effect of the H520C9sFv-rhIL-2 in preventing the establishment of metastatic tumors in SCID mice.

CHAPTER 2

Literature Review

2.1 Interleukin-2

2.11 Biological Characteristics of IL-2

Human Interleukin-2 (IL-2) is a 15 kD glycoprotein, originally named T-cell growth factor (TCGF) and produced by T lymphocytes. It is encoded by a single gene on human chromosome 4 which produces a 133-amino-acid polypeptide (Oppenheim and Lotze, 1994). IL-2 has been found to support T-cell proliferation, augment natural killer (NK) cell cytotoxicity, induce lymphokine-activated killer (LAK) cell development and participate in the activation of monocytes and B cells (Whittington and Faulds, 1993). In addition, IL-2 can enhance production of interferon-gamma (INF-γ), tumor necrosis factor (TNF), IL-1 and IL-6 (Maas et al, 1993). These properties suggest that IL-2 could be effective in stimulating the host immune response for the treatment of cancers.

2.12 Clinical Application of IL-2 in Cancer Treatment

Due to the fact that IL-2 has the ability to support the proliferation and activation of numerous types of immune lymphoid cells, there has been considerable research in its use in immunotherapy of cancers. IL-2 has a short in vivo serum half-life of 3.7 min. in mice and 6.9 min. in human after intravenous injection (Donohue and Rosenberg, 1983 and Lotze et al, 1986). The rapid elimination of IL-2 from blood stream by the kidney, however, has severely limited its utility. Thus, high doses of systemically administrated IL-2 are necessary for substained levels in the circulation in order to obtain anti-tumor responses. Extensive research reported that the systemic administration of high doses IL-2, either alone or in conjugation with immune lymphoid cells could result in the regression of metastatic cancer in animal models and patients with melanoma and renal cell carcinoma (Dillman 1999, Baars et al 1992, Rosenberg et al 1989, Lotze et al 1986, Lafreniere and Rosenberg 1985). The antitumor efficacy of IL-2 was directly related to the injected dose level. However, the systemic administration of high doses IL-2 caused severe toxic side effects. The side effects are presented as fever, chills,

malaise, arthralgias, myalgias and weight gain related to marked fluid retention. The most frequent and serious adverse effect of IL-2 is the vascular leak syndrome, characterized by damage to the endothelial cells with extravasation of plasma proteins and fluid from capillaries into the extravascular space (Vial and Descotes, 1992, Siegel and Puri, 1991). Much effort has been made to reduce the dose-limiting toxicities and improve the tolerability of systemic IL-2 therapy. Some studies have shown that intratumoral injection of low doses IL-2 could be effective against cancer without toxic side effects and could stimulate a specific anti-tumor immune response (Mass et al, 1991 and Lotze et al, 1986). However, not all tumors are easily accessible for local injection due to the tumor size and location. Additionally, the injected IL-2 remained at the tumor site only for a short period of time before diffusing into blood stream decreasing its effectiveness. In order to overcome the limitations of systemic use of IL-2 in cancer treatment, an alternative approach for achieving effective local concentration of IL-2 has been developed. Recombinant antibody-IL-2 fusion proteins were developed which combine the unique tumor-specific targeting ability of antibody with the multifunctional activity of IL-2.

2.2 Immunotherapy by Means of Antibody-IL-2 Fusion Proteins

The use of recombinant antibody-IL-2 fusion proteins for cancer immunotherapy has several advantages. First of all, the variable region of antibody can specifically target to its tumor associated antigens and result in concentrating the localized dose of IL-2 at the tumor. Secondly, the short in vivo half-life of the IL-2 can be extended due to the increased size of the recombinant antibody-IL-2 conjugate and inherent stability of the antibody. Thirdly, extensive research studies demonstrated that recombinant antibody-IL-2 fusion proteins could induce an immune response capable of eradicating established cancer metastases in animal tumor models (Hornick et al, 1999, Melani et al, 1998, Xiang et al, 1997 and Becker et al, 1996). The anti-tumor effect has been demonstrated with ch14.18-IL-2, KS1/4-IL-2 and chS5A8-IL2 fusion proteins in 4 syngeneic tumor models for neuroblastoma (Lode et al, 1998), melanoma (Becker et al, 1996, and Sabzevari et al, 1994), colon carcinoma (Xiang et.al, 1994) and B cell lymphoma (Penichet et al, 1998).

2.3 HER-2/*neu*

2.31 Biology of HER-2/*neu*

HER-2/*neu*, also known as c-erbB-2, is the second member of the epidermal growth factor family (Szollosi et al, 1995 and Yu et al, 1993). It encodes for a 185 kDa transmembrane glycoprotein, p185, with tyrosine kinase activity. p185 is homologous to the human epidermal growth factor receptor (Hung et al, 1999 and Fendly et al, 1990). This receptor is expressed on the plasma cell membrane of a variety of epithelial cell types and regulates cell growth and division through binding of specific growth factors.

2.32 Role of HER-2/*neu* in Cancer

While HER-2/*neu* is expressed at low levels in many normal cells, it is overexpressed in a variety of cancers. Overexpression of HER-2/*neu* by gene amplification confers a more aggressive behavior on tumors and results in significantly shorter time to relapse and survival times when compared to patients without HER-2/*neu* overexpresssion

(Pegram et al, 1998 and Carter et al, 1992). In addition, amplification and/or overexpression of HER-2/*neu* is associated with poor prognosis of multiple human cancer types, including breast, ovarian, endometrial, gastric, pancreatic, prostate and salivary gland. (Reese and Slamon, 1997, Meden and Kuhn, 1997, Cirisano and Karlan, 1996).

2.33 HER-2/*neu* in Breast and Ovarian Cancers

Research studies have shown that overexpression of HER-2/*neu* plays a direct role in the pathogenesis and aggressiveness of approximately 30% of invasive human breast and ovarian cancer tumors (Toikkansen et al, 1992, Ring et al, 1991, Tandon et al, 1989). Furthermore, amplification and overexpression of the HER-2/*neu* proto-oncogene were recognized as an adverse prognostic factor for both primary, metastatic breast and ovarian cancers (Wong et al, 1995).

2.34 HER-2/*neu* as a Therapeutic Target

Many studies have convincingly shown that repression of HER-2/*neu*

suppressed the malignant phenotypes of HER-2/*neu* overexpressing cancer cells. These findings strongly suggested that HER-2/*neu* might serve as an excellent target for developing anti-cancer agents specific for active immunotherapy (Yu et al, 1993).

2.4 Recombinant Antibody-IL-2 Fusion Protein for HER-2/*neu* Overexpressed Tumor

A cDNA encoding for a recombinant humanized single-chain Fv (sFv) antibody-IL-2 fusion protein directed against the HER-2/*neu* proto-oncogene product, p185, has been constructed by combining the cDNA of a humanized sFv of a murine monoclonal antibody (520C9) and the cDNA of recombinant human IL-2. Human embryonic kidney 293 cells were used for stable expression of the cDNA encoding the antibody-IL-2 fusion protein, H520C9sFv-rhIL-2. The H520C9sFv-rhIL-2 has been characterized to retain both the immunostimulatory effects of IL-2, as shown by IL-2 dependent cell proliferation and cytotoxicity assays, and full binding activity against the HER-2/*neu* (c-erbB2) proto-oncogene product, p185, as determined by ELISA (Li et al, 1999).

The anti-tumor efficacy of the H520C9sFv-rhIL-2 in C57 BL/6 mice carrying subcutaneous syngeneic tumors and human HER-2/*neu* cDNA was reported (Kwok et al, 2001). The results demonstrated that the fusion protein could inhibit the growth of HER-2/*neu* positive tumors in immuno-competent animals. However, the therapeutic effect of the H520C9sFv-rhIL-2 in animals with metastatic HER-2/*neu* positive tumor remains to be established.

CHAPTER 3

Materials and Methodology

3.1 Tumor Cell Line

The HER-2/*neu* positive SKOV3 cell line, derived from a human adenocarcinoma of ovary, was obtained from the Department of Pathology, McMaster University, Hamilton, Ontario, Canada. The cell line was maintained as a monolayer in RPMI 1640 (Gibco BRL) supplemented with 15 % Fetal Calf Serum (FCS from Gibco BRL) and a 2% Penicillin-Streptomycin antibiotic mixture (Gibco BRL) at 37^0C under 5% CO_2 in an incubator.

3.2 Nude & Severe Combined Immuno-Deficiency (SCID) Mice

Female BALB/c nude and nod-SCID mice were obtained from The Radiobiology Lab, Clinical Oncology Department, Queen Elizabeth Hospital. The mice were maintained under pathogen-free conditions in a laminar flow rack and used for experiments when they were 7 weeks old. They were fed with sterilized mouse diet and water.

3.3 Expression and Purification of H520C9sFv-rhIL-2

Human embryonic kidney 293 cells transfected with the cDNA of H520C9sFv-rhIL-2 (Li, 1999) were grown at 37^{0}C in DMEM (Gibco BRL) supplemented with 10% FCS and 8 μg/ml of Geneticin Selective Antibiotic (Life Technologies). The H520C9sFv-rhIL-2 consisted of a recombinant human IL-2 and a recombinant humanized single chain antibody which combined the V_H and V_L portions of a murine monoclonal antibody (520C9). When the 293 cells were grown to near 50% confluency, the cells were washed with serum free DMEM (Gibco BRL) thoroughly for two times. Then, the 293 cells were resuspended with the serum free DMEM (Gibco BRL) at 37^{0}C under 5% CO_2 in an incubator. When the 293 cells were grown to 90% confluency, spent cultured media were collected from the culture. The collected conditioned media were concentrated 50-folds with the use of a centrifuge tube concentrator with 30,000-dalton exclusion limit (Millipore Corp., Bedford, MA). The concentrated conditioned media were purified to remove Geneticin Selective Antibiotic with a seamless cellulose dialysis tubing (Sigma Chemical, USA) in a changing buffer of 0.9% NaCl.

3.4 SDS-PolyAcrylamide Gel Electrophoresis (SDS-PAGE) and Western Blotting Analysis

Protein samples from the concentrated conditioned media were solubilized at 95^{0}C for 5 min. in a sample buffer containing 0.5 M Tris HCl at pH6.8 and 10% SDS (w/v) and then loaded onto polyacrylamide gels. Electrophoresis was performed in a 1mm-thick 12% SDS (w/v) separating gel topped with 4% stacking gel for 1.5 hr. under 180V, with a Tris-glycine buffer system in an electrophoresis unit. Thereafter, proteins on the gel were visualized by silver staining (Amity, Amersham Life Science). In order to immunoprobe the IL-2 component of the H520C9sFv-rhIL-2, the embedded proteins in polyacrylamide gel after electrophoresis were transferred to a nitrocellulose membrane (Bio-Rad, Hercules, Calif.) using standard technique. A mouse anti-human IL-2 antibody MAB202 (Research & Diagnostics Systems, Minneapolis, MN), diluted at 2.5 μg/ml in TBST with 5% (v/v) non-fat dried milk powder, was added and incubated for 2 hr. at 37^{0}C. The membrane was then incubated with a goat anti-mouse IgG antibody coupled to horseradish peroxidase (DAKO, Copenhagen, Denmark) for 1 hr., which had been diluted to a

concentration of 2 μg/ml in TBST with 5% (v/v) non-fat dried milk powder. After three washes, the membrane was tested with chemiluminescence detection solutions (Santa Cruz, Carpinteria, Calif) and exposed to Hyperfilm (Amity, Amersham Life Science) from 10 sec. to 5 min.

3.5 Determination of the Antigen Binding Specificity of H520C9sFv-rhIL-2

The specific antigen binding activity of the H520C9sFv-rhIL-2 was examined by cell mediated ELISA using HER-2/*neu* positive SKOV3 cells and HER-2/*neu* negative HeLa cells as negative control. C8 Maxisorp Nunc Immunomodules (Nunc, Roskilde, Denmark) were coated overnight at 37^0C with 1 x 10^4 live SKOV3 and HeLa cells in 100 μl culture medium per well separately. Serially diluted samples of the H520C9sFv-rhIL-2 were then added to each well of the plate and incubated at 37^0C for 2 hr. After three washes with PBS containing 0.05% Tween-20 (PBST), 100 μl (1:200 dilution) of MAB202 (Research & Diagnostics Systems, Minneapolis, MN) was added to each well and incubated for 2 hr. Following three washes with PBST,

100 µl goat anti-mouse polyclonal antibody (DAKO) (1:6000 dilution) conjugated with horseradish peroxidase was added to each well. After 2 hr. incubation, the cells were washed three times with PBST and followed by 100 µl of 1 mM H_2S0_4, colour was developed with the addition of 100 µl peroxidase substrate (Bio-Rad. Hercules, CA) and the resulting OD was determined at 450nm in a microplate reader.

3.6 Determination of the IL-2 Moiety in H520C9sFv-rhIL-2

ELISA was performed to examine the presence of IL-2 moiety in H520C9sFv-rhIL-2. Wells of an ELISA plate were coated overnight at 37^0C with serially diluted samples of the H520C9sFv-rhIL-2 and standard samples of IL-2. After three washes with PBS, the plate was incubated with 100 µl (1:200 dilution) mouse anti-human IL-2 antibody MAB202 (Research & Diagnostics Systems, Minneapolis, MN`) at 37^0C for 2 hr. The plate was then washed three times with PBS, followed by the addition of 100µl goat anti-mouse polyclonal antibody (DAKO) (1:6000 dilution) conjugated with horseradish

peroxidase per well for 1 hr. at 37^{0}C. After three additional washes with PBS, colour development was performed with incubation of 100 µl peroxidase substrate (Bio-Rad) per well and the resulting OD was determined at 450nm in a microplate reader.

3.7 Preparation of Human Peripheral Blood Mononuclear (PBM) Cells

Human peripheral blood mononuclear cells were isolated from the blood of a healthy donor by Ficoll-Hypaque density gradient centrifugation. 25ml of fresh heparinized blood was mixed well with equal volume of PBS in a conical centrifuge tube at room temperature. Then, the Ficoll-Hypaque solution was layered carefully underneath the blood/PBS mixture with a sterile pipet. The centrifuge tube was centrifuged at 1850 RCF(g) for 8 min. with no brake. The buffy coat layer was collected, washed with RPMI 1640 three times and spun at 260 RCF(g) for 5 min. each time after washing. Finally, the peripheral blood mononuclear cell suspension was resuspended in RPMI 1640 to the appropriate concentrations. The cell viability as assessed by trypan blue exclusion exceeded 95% in all preparations.

3.8 Experimental Model of Tumor Metastases in Lungs of Nude and SCID Mice

SKOV3 cells were dispersed from culture flasks by brief exposure to a Trypsin-EDTA solution consisting of 0.5 g of trypsin (1:250) / liter and 0.2 g of EDTA / liter in Hanks' balanced salt solution without calcium or magnesium. Cell suspensions were centrifuged and resuspended in RPMI 1640 to the appropriate concentrations. Cell viability exceeded 95% in all preparations. A single cell suspension of 3.5×10^6 SKOV3 tumor cells for a nude mouse and 4×10^6, 6×10^6 or 8×10^6 SKOV3 tumor cells for SCID mice were injected intravenously and slowly via a lateral tail vein with a 29-G needle (Terumo) in 0.2ml of RMPI 1640.

3.9 Intraperitoneal Tumor Model in Nude and SCID Mice

Single cell suspensions of 6 x 10^6 or 8 x 10^6 SKOV3 tumor cells for nude mice as well as 3 x 10^6 or 6 x 10^6 SKOV3 tumor cells for SCID mice were injected slowly by using a 29-G needle into the peritoneum of each mouse in 0.2 ml of RPMI 1640. The mice were housed separately during subsequent tumor growth and any grossly visible changes of abdominal cavities were recorded each week.

3.10 Subcutaneous Tumor Model in Nude Mice

Single cell suspensions of 2.5 x 10^6, 5 x 10^6 or 10 x 10^6 SKOV3 tumor cells in 0.2 ml of RMPI 1640 were injected s.c. in the midabdominal flank of three nude mice respectively at 2 locations, one at the upper flank and the other at the lower flank. The mice were housed separately during subsequent tumor growth. The maximum growth dimension of the established tumor was estimated by weekly measuring with a caliper the maximum tumor length, width and depth in orthogonal directions.

3.11 Immunotherapy Protocol in Subcutaneous Model

7-week-old SCID mice were randomly assigned into 3 groups of 2. Each SCID mouse was injected s.c. at the back just behind the neck with 2 x 10^6 SKOV3 tumor cells in 0.2ml physiological saline. Every day from Day 4 to Day 10 after tumor cell inoculation, 0.2ml each of 3 different treatment agents was injected s.c. to the tumor cell inoculation site. The compositions of the treatment agents for the 3 groups were as follows:

	Group A	Group B	Group C
Treatment Agents	2 μg H520C9sFv-rhIL-2 + PBM cells.	Saline + PBM cells.	Saline only.

PBM cells = 5 x 10^6 fresh human peripheral blood mononuclear cells from a healthy donor. The mice were monitored every two days for tumor size post tumor cell inoculation.

3.12 Immunotherapy Protocol in Metastatic Model

3.121 Experiment 1

7-week-old SCID mice were randomly assigned into 4 groups of 4. Each SCID mouse was injected intravenously with 8 x 10^6 SKOV3 tumor cells in 0.2 ml of RMPI 1640. Every day from Day 4 to Day 6 after tumor cell inoculation, 0.2ml each of 4 different treatment agents was injected intravenously via one of its lateral tail veins into each mouse. The compositions of the treatment agents for the 4 groups were as follows:

	Group A	Group B	Group C	Group D
Treatment Agents	6 μg H520C9sFv-rhIL-2 + PBM cells.	6 μg H520C9sFv-rhIL-2 only.	PBM cells only.	Saline only.

PBM cells = 0.2 x 10^6 fresh human peripheral blood mononuclear cells from a healthy donor. On Day 28 after tumor cell inoculation, each group of mice was sacrificed to determine the therapeutic effect of the fusion protein in generating anti-tumor response.

3.122 Experiment 2

7-week-old SCID mice were randomly assigned into 3 groups of 8. Each SCID mouse was injected intravenously with 8 x 10^6 SKOV3 tumor cells in 0.2 ml of RMPI 1640. Every day from Day 4 to Day 6 after tumor cell inoculation, 0.2 ml each of 3 different treatment agents was injected intravenously via one of its lateral tail veins into each mouse. The compositions of the treatment agents for the 3 groups were as follows:

	Group A	Group B	Group C
Treatment Agents	6 μg H520C9sFv-rhIL-2 + PBM cells.	3 μg H520C9sFv-rhIL-2 + PBM cells.	Saline only.

PBM cells = 0.2 x 10^6 fresh human peripheral blood mononuclear cells from a healthy donor. On Day 14 and Day 28 after tumor cell inoculation, each group of 4 SCID mice was sacrificed to determine the therapeutic effect of the fusion protein in generating anti-tumor response.

3.13 Histological Examination of Metastatic Lung Tissue

A piece of lung tissue was excised from each sacrificed SCID mouse after treatment for lung metastases and fixed in formalin solution immediately after dissection. The complete fixation required 12 to 24 hr. at room temperature. The fixed lung tissue was then processed in a Shandon Citadel Automated Tissue Processor for dehydration, clearing and embedding in paraffin wax. 5 μm thick slides were cut from the tissue block and mounted on microscopic slides for haematoxylin and eosin staining. Nuclear and cytoplasmic details of the cells in the tissue slides were examined under a microscope equipped with a digital camera. For immunohistochemistry of frozen lung tissues from each sacrificed SCID mice after treatment for lung metastases, a piece of lung tissue was carefully embedded in frozen tissue matrix O.C.T. (Finetek, USA) in an aluminium foil mold. Then, the mold was put into -70^{0}C freezer until ready for sectioning. Upon cutting sections, the frozen tissue block was allowed to equilibrate in the cryostat chamber for 5 min. at -20^{0}C. 5 μm thick slides were cut from the frozen tissue block and mounted on microscopic slides.

Thereafter, the tissue sections in slides were fixed in cold acetone for 2 min. at room temperature and ready for immunohistochemical staining after air dry.

3.14 Immunohistochemical Analysis of HER-2/*neu* Protein in Metastatic Lung Tissues of SCID mice

The 5 μm thick formalin-fixed tissue section slides were deparaffinized in 2 changes of xylene for 15 min. each and then transferred to 2 changes of absolute alcohol for 15 min. each. Following a 15 min. incubation with a Proteinase K (Boehringer Mannheim) working solution, the sections were incubated for 2 hr. at room temperature with a primary antibody anti-HER-2/*neu* FITC (BD Biosciences) diluted 1:20 with antibody diluent (DAKO). Following a 5 min. wash in TBS/Triton, the sections were treated for 30 min. with a secondary Rabbit F(ab') anti-FITC/AP antibody (DAKO) diluted 1:50 with BSA buffer followed by a 5 min. wash in TBS/Triton. The slides were then immersed in a BCIP/NBT substrate solution (DAKO) for 30 min., followed by a 10 min. rinse with running tap water. Thereafter, the sections were examined by visible light microscopy for the presence of dark brown staining.

3.15 Indian Ink Staining of Lungs with Metastatic Tumor Nodules in SCID mice

The lungs of each sacrificed SCID mouse after treatment for lung metastases were removed by opening the thoracic cavity, injected with 2 ml of a 15% solution of Indian ink (Cancer Diagnostic, Inc., Birmingham, MI) into the trachea and bleached with Fekette's solution immediately for 24 hr. at room temperature. The Fekette's solution composed of 5 ml glacial acetic acid, 10 ml formaldehyde and 100 ml of 70% alcohol. The area percentage occupied by white tumor nodules on the black lung surface was counted with the use of OPTIMAS 6.0™ image analysis software.

3.16 Statistical Analysis

One-way ANOVA test and post hoc Scheffe test were used to determine the statistical significance of differential findings and group mean differences in percentage area of lungs surface covered by metastatic foci between various experimental groups of SCID mice respectively. The statistical findings were regarded as significant if p values were < 0.05.

CHAPTER 4

Results

4.1 Expression of the H520C9sFv-rhIL-2

Culture supernatant media from human embryonic kidney 293 cells transfected with the cDNA of the H520C9sFv-rhIL-2 were collected, concentrated 50-folds and then analyzed by SDS-PAGE and visualized using silver staining. Although the expected band for the H520C9sFv-rhIL-2 was fairly broad as shown in Fig. 1., Western blotting analysis was also performed to confirm the expected molecular weight of the H520C9sFv-rhIL-2. As shown in Fig. 2., IL-2 was shown as a band of 15 kDa and IL-2 dimer as a 30 kDa band in Lane A. In addition, a single band of 45 kDa was observed in the conditioned media (Lane B) and correlated with the expected molecular weight of the H520C9sFv-rhIL-2. The existence of a 30 kDa band in Lane B indicated the existence of a protein with molecular weight of 30kDa and IL-2 dimer. This protein could be a fragment of the fusion protein containing IL-2 or an IL-2 dimer. The results demonstrated that the transfected human embryonic kidney 293 cells stably expressed the H520C9sFv-rhIL-2.

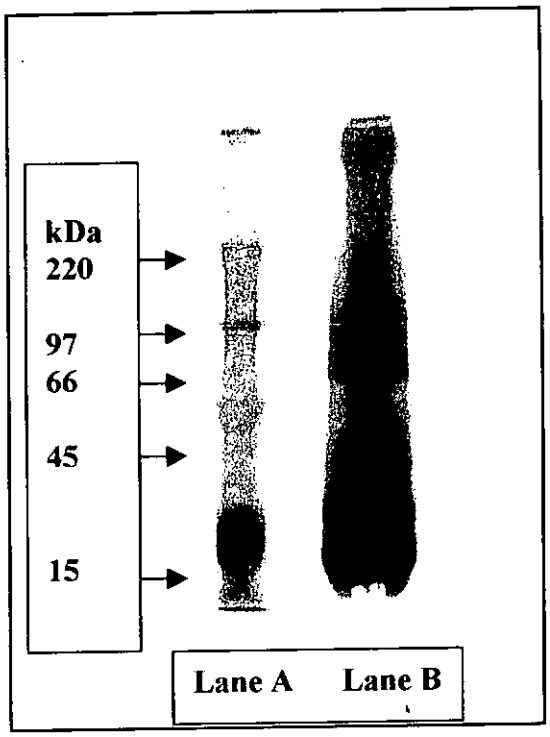

Fig. 1. SDS-PAGE analysis of the H520C9sFv-rhIL-2. Lane A. Low molecular weight rainbow markers. Lane B. 10 µl of concentrated, conditioned media from 293 cells transfected with the cDNA of the H520C9sFv-rhIL-2.

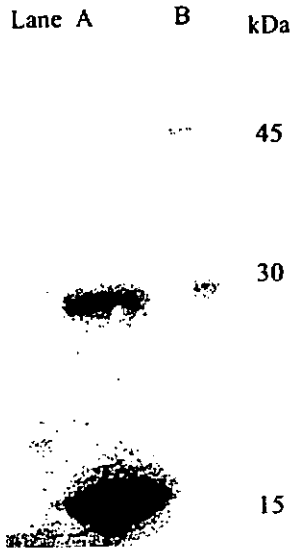

Fig. 2. Western blot analysis of IL-2 contained in H520C9sFv-rhIL-2 in culture conditioned media from transfected 293 cells. Lane A. 5µg of IL-2. Lane B. 10 µl of the concentrated, conditioned media.

4.2 Determination of the Antigen Binding Specificity of H520C9sFv-rhIL-2

The specific antigen binding activity of the H520C9sFv-rhIL-2 was determined using indirect cellular ELISA on SKOV3 cells, which overexpressed the p185. In Fig. 3., the conditioned media containing the H520C9sFv-rhIL-2 displayed binding activity for the SKOV3 cells but less binding activity for p185 negative HeLa cells. In a positive control cellular ELISA as shown in Fig. 4., the anti-p185 520C9 monoclonal antibody was demonstrated to bind to the p185 overexpressed SKOV3 cells, but not to the HeLa cells.

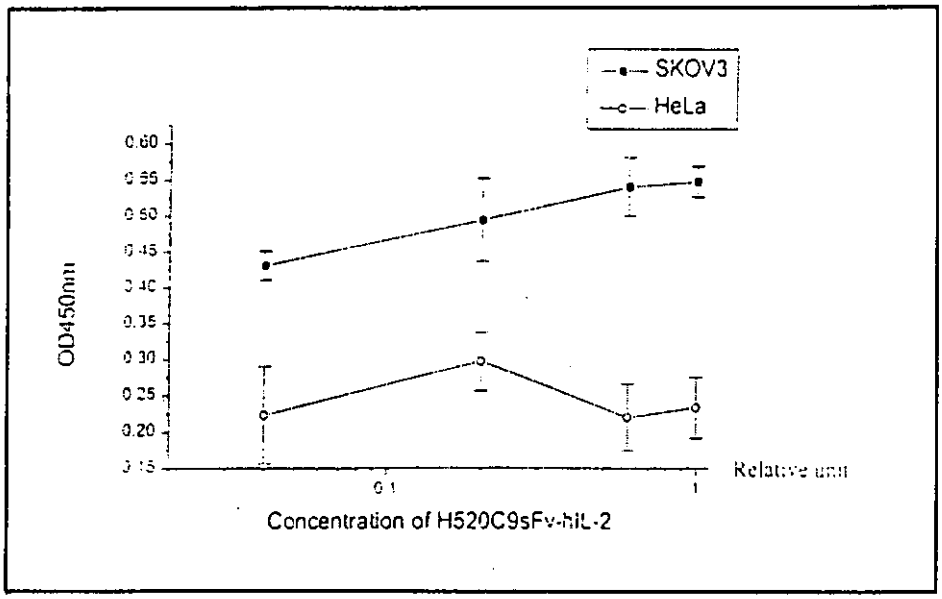

Fig. 3. Determination of the H520C9sFv-rhIL-2 for the p185 antigen binding activity by indirect ELISA using cultured SKOV3 cells. The H520C9sFv-rhIL-2 with serial dilution as indicated from the original concentrated supernatant was shown to bind to p185 positive SKOV3 cells, but not p185 negative HeLa cells. The error bars show ± one standard deviation.

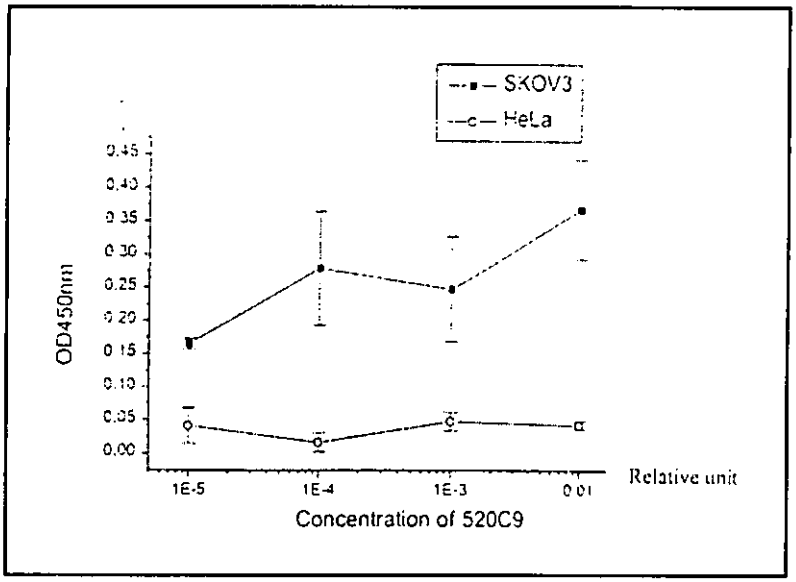

Fig. 4. Determination of the p185 antigen binding activity of parental monoclonal antibody 520C9. The parental monoclonal antibody 520C9 with serial dilution of 10-folds from the original concentration showed specific antigen binding to p185 positive SKOV3 cells, but not to p185 negative HeLa cells. The error bars show ± one standard deviation.

4.3 Determination of the Concentration of IL-2 Moiety in H520C9sFv-rhIL-2

The presence of IL-2 moiety in conditioned media from 293 cells transfected with the cDNA of the H520C9sFv-rhIL-2 was identified by ELISA using a mouse anti-human IL-2 monoclonal antibody MAB202. The measured OD for serially diluted standard samples of IL-2 were shown in Fig. 5. As shown in Fig. 6, the measured OD increased as the relative concentration of the H520C9sFv-rhIL-2 increased accordingly. However, there was a decrease in the measured OD when the relative concentration of H520C9sFv-rhIL-2 was over 1. The monoclonal antibody MAB202 was demonstrated to bind to the IL-2 portion of the H520C9sFv-rhIL-2 and possibly to the IL-2 containing component present in the conditioned media.

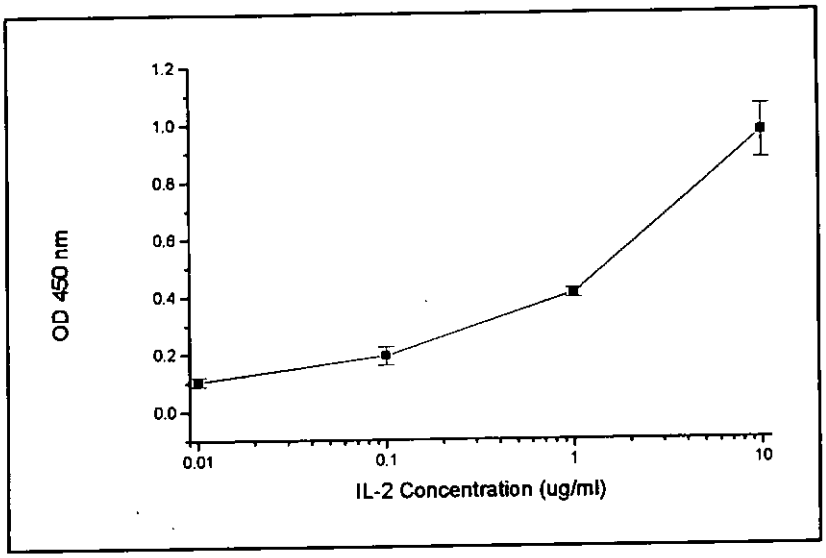

Fig. 5. The IL-2 absorbance of standard samples of human IL-2 serially diluted 10-folds from the original concentration. The error bars show ± one standard deviation.

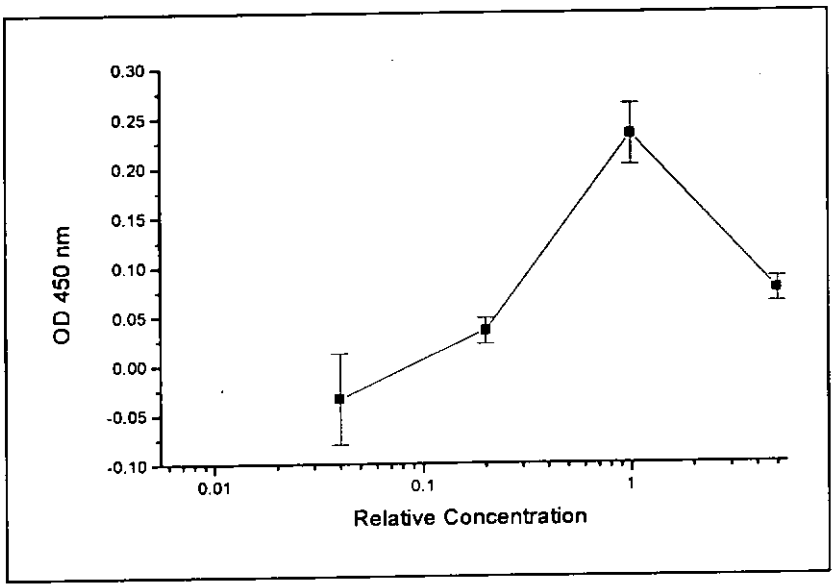

Fig. 6. The IL-2 absorbance of samples of conditioned media serially diluted 5-folds from the original concentrated medium from 293 cells transfected with the cDNA of the H520C9sFv-rhIL-2. The error bars show ± one standard deviation.

4.4 Establishment of Experimental Tumor Models

In order to evaluate the therapeutic effect of the H520C9sFv-rhIL-2 against human HER-2/*neu* positive tumor *in vivo*, several experimental tumor models were established using HER-2/*neu* overexpressing SKOV3 ovarian carcinoma cells in mice.

4.41 Subcutaneous Tumor Model in Nude Mice

Three nude mice (n=3) were injected subcutaneously with 2.5 x 10^6, 5 x 10^6 or 10x10^6 SKOV3 tumor cells respectively. Each of the 3 nude mice was injected with SKOV3 tumor cells at 2 locations, one at the upper flank region and the other at the lower flank region, subcutaneous tumor nodules were measurable 2 weeks post tumor cell inoculation as shown in Fig. 7. The measured volumes of the subcutaneous tumor nodules in each of 3 nude mice were summarized in Fig. 8. Drastic increases in size of the tumor nodules were observed in nude mice 1 month after injection with 2.5 x 10^6 SKOV3 cells. Central necrosis of the subcutaneous tumor nodule was observed as shown in Fig. 9. Moreover, the tumor nodule was infiltrated with blood vessels and surrounded by a capsule of connective tissue as shown in Fig. 10 and Fig. 11. Upon histological staining with haematoxylin &

eosin, the SKOV3 tumor nodule section revealed prominent nuclei and an irregular cell pattern as shown in Fig. 12. The nude mouse injected with 10 x 10^6 SKOV3 cells could only tolerate the tumor load for around 1 month, followed by severe necrosis of the tumor nodules and the mouse die from tumor burden about 1 month after tumor cell injection.

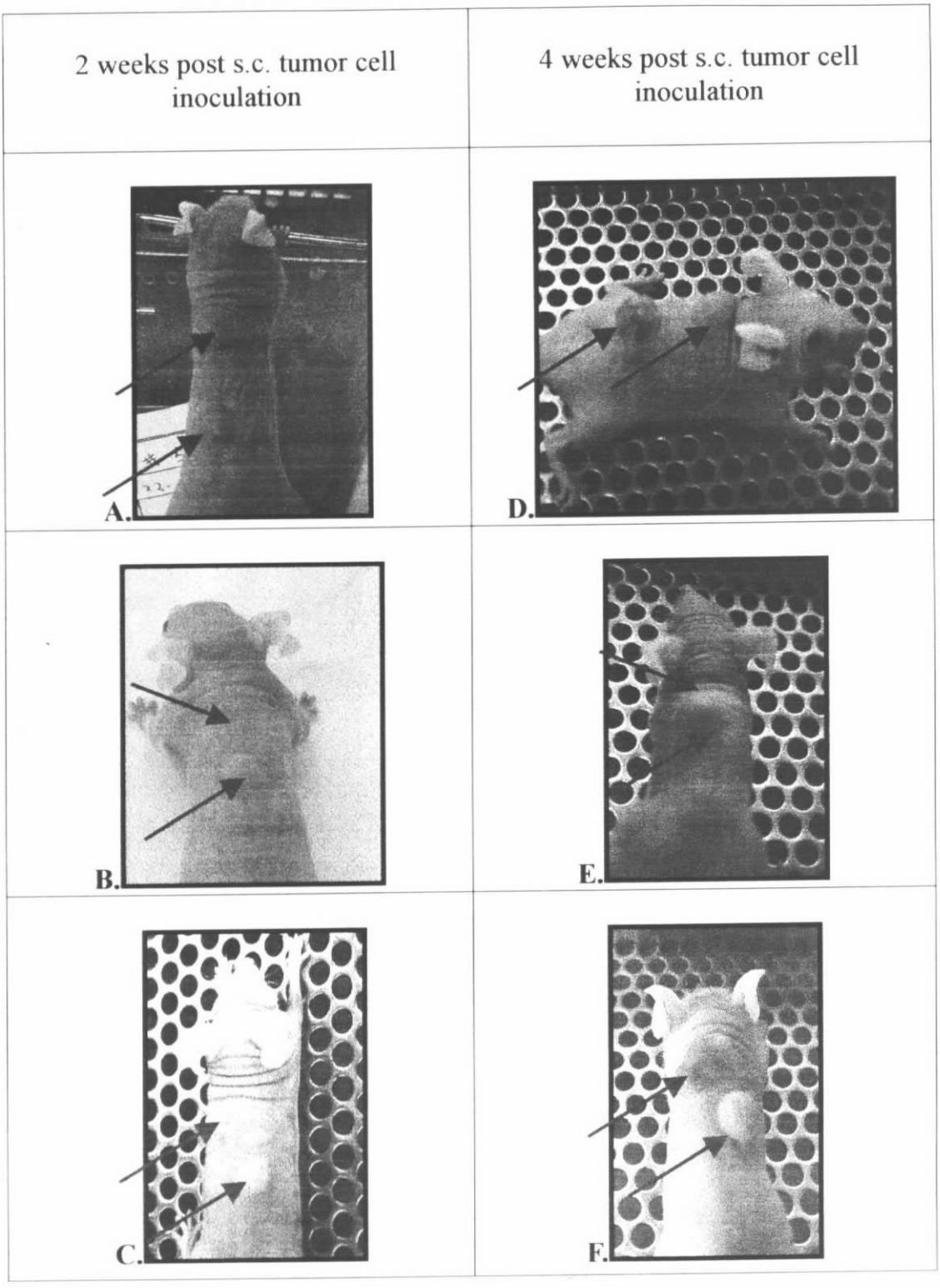

Fig. 7. Appearance of tumor nodules indicated by arrows 2 weeks after subcutaneous injection of 2.5 x 10^6 SKOV3 cells (panel A), 5 x 10^6 SKOV3 cells (panel B) or 10 x 10^6 SKOV3 cells (panel C) to each of 3 nude mice at 2 locations respectively. Increased sizes (panels D, E & F) were observed in the mice after 4 weeks.

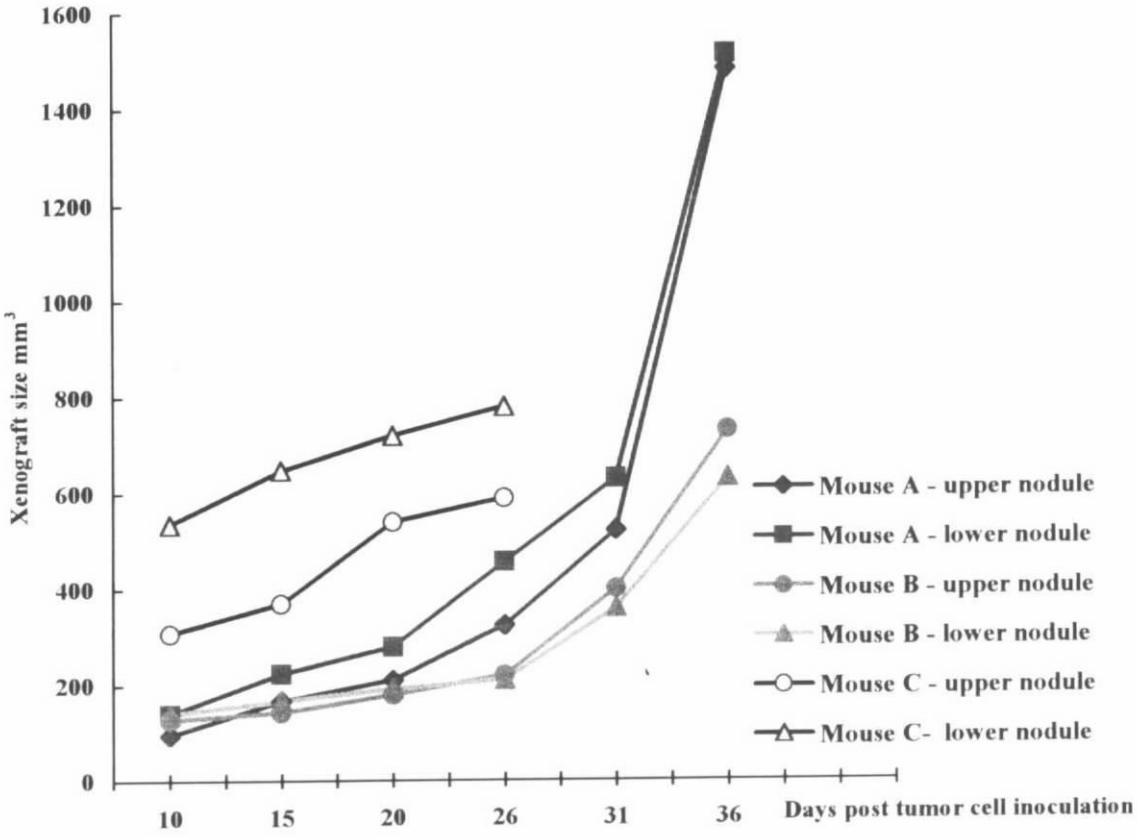

Fig. 8. The measured sizes of subcutaneous SKOV3 xenograft tumor nodules in nude mice at various days after injection with 2.5 x 10^6 (mouse A), 5 x 10^6 (mouse B) or 10 x 10^6 (mouse C) SKOV3 cells.

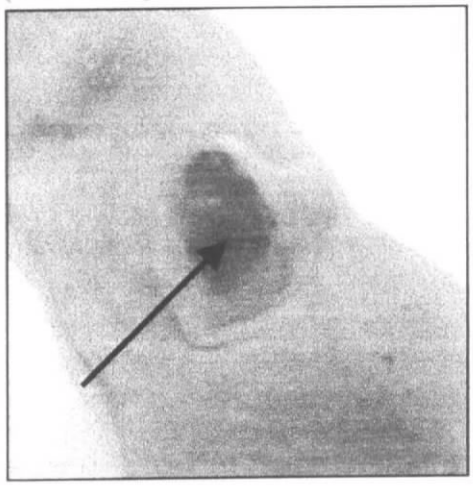

Fig. 9. The subcutaneous tumor nodule was observed to be necrotic (indicated by arrow) 1 month after s.c. injection of 2.5 x 10^6 SKOV3 tumor cells.

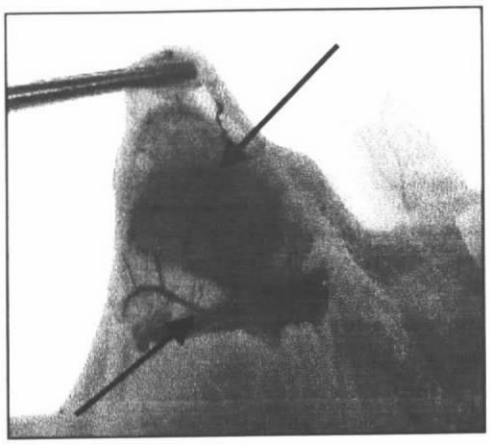

Fig. 10. An extensive blood vessel network was developed indicated by arrows around the subcutaneous tumor nodule 1 month after s.c. injection of 2.5 x 10^6 SKOV3 tumor cells.

Fig. 11. The freshly excised subcutaneous tumor nodule was surrounded by a capsule.

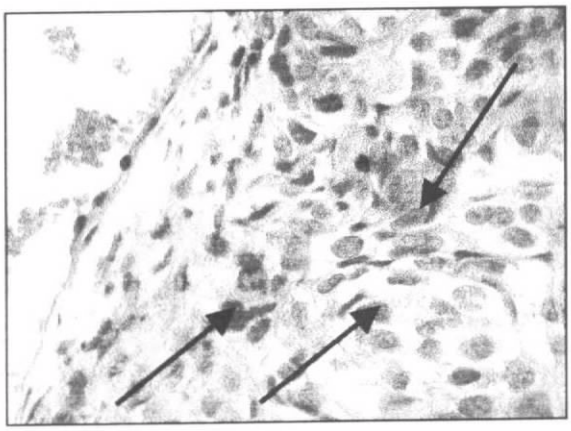

Fig. 12. Formalin-fixed SKOV3 tumor nodule was subjected to paraffin embedding and subsequent haematoxylin & eosin staining. Prominent nuclei and an irregular cell pattern of SKOV3 cells as indicated by arrows were observed. Representative area was photographed at a magnification of x 360.

4.42 Intraperitoneal Tumor Model in Nude Mice

Severe bloody ascites and peritoneal dissemination of SKOV3 tumor nodules were observed in nude mice 3 weeks after i.p. injection of 6 x 10^6 or 8 x 10^6 SKOV3 cells as shown in Fig. 13. In addition, the disseminated tumors were mainly observed in the mesenterium and invasive growth into the liver capsule was also noted as shown in Fig. 14 and Fig. 15 respectively.

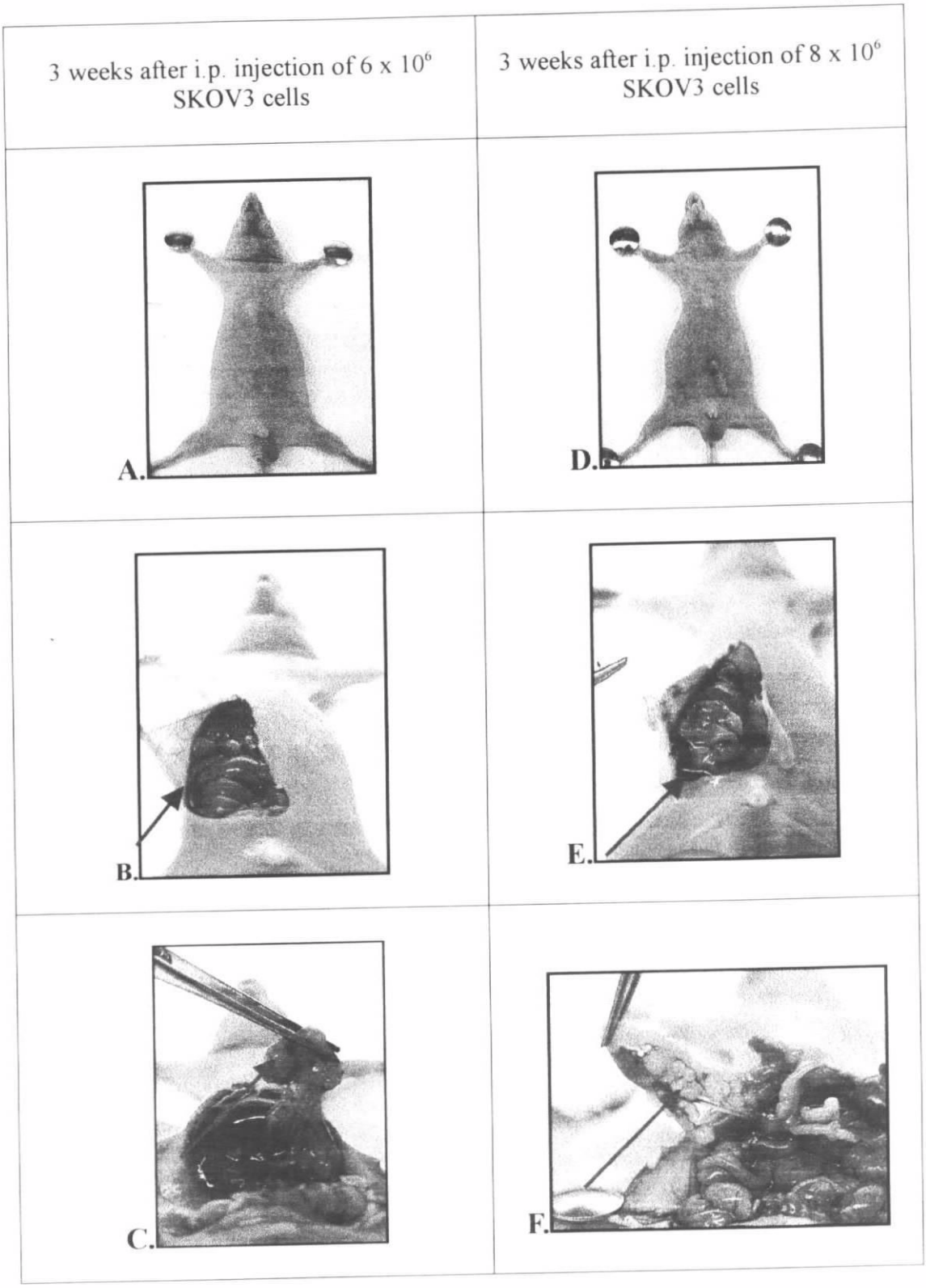

Fig.13. 3 weeks after intraperitoneal injection of 6 x 10^6 SKOV3 cells (panel A, B & C) or 8 x 10^6 SKOV3 cells (panel D, E & F) to each of 2 nude mice respectively, extensive abdominal ascites (panel B, E) and tumor growth (panel C, F) were observed in both nude mice upon abdominal dissection as indicated by arrows.

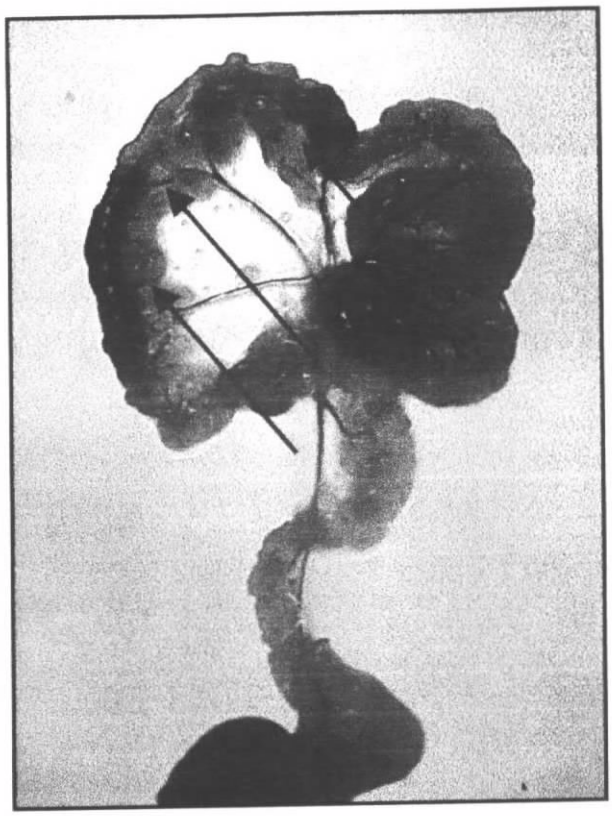

Fig. 14. Macroscopic observation of abdominal organs 3 weeks after i.p. injection of 8 x 10^6 SKOV3 cells in a nude mouse. Multiple white tumor nodules were apparent on the mesenterium as indicated by arrows.

Fig. 15. An invasive growth of SKOV3 tumor cells into the liver capsule was observed as indicated by arrow in a nude mouse 3 weeks after i.p. injection of 8 x 10^6 SKOV3 cells.

4.43 Intraperitoneal Tumor Model in SCID Mice

Extensive peritoneal dissemination of SKOV3 tumor nodules within the mesenterium were also observed in SCID mice 3 weeks after i.p. injection of 3 x 10^6 or 6 x 10^6 SKOV3 cells as shown in Fig. 16.

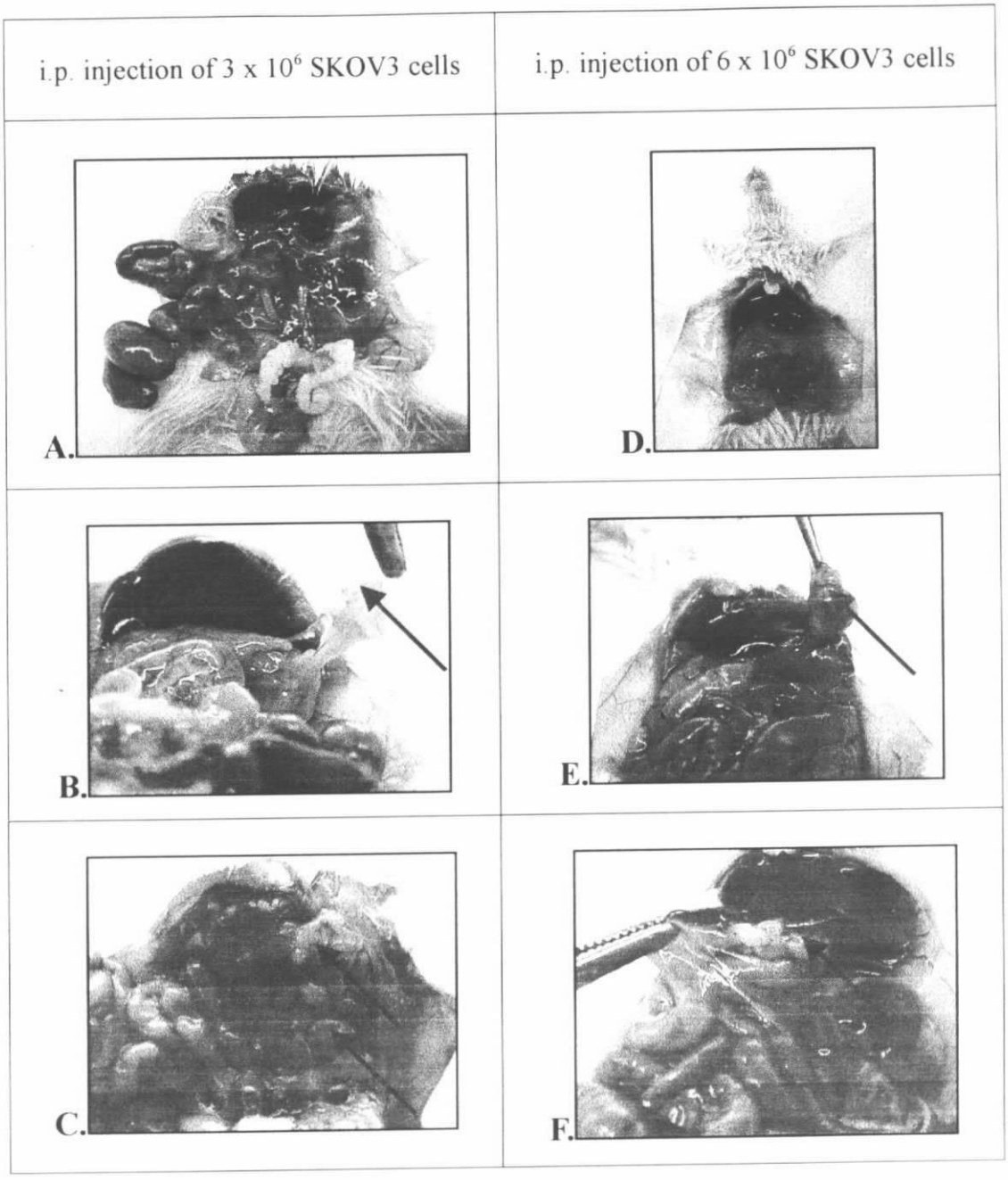

Fig.16. No ascites were observed 1 week after intraperitoneal injection of 3 x 10^6 SKOV3 cells (panel A) or 6 x 10^6 SKOV3 cells (panel D) in each of 2 SCID mice respectively. Growth of tumor nodules were observed within the abdominal cavities of the SCID mice 2 weeks after tumor cells inoculation (panel B and E) as indicated by arrows. Also, extensive abdominal tumor nodules (panel C and F) were developed in both SCID mice upon abdominal dissection 3 weeks after tumor cells inoculation as indicated by arrows.

4.44 Intravenous Tumor Model in Nude and SCID Mice

4 weeks after intravenous injections of 3.5 x 10^6 SKOV3 tumor cells via a lateral tail vein into a nude mouse and 4 x 10^6, 6 x 10^6 or 8 x 10^6 SKOV3 cells into several SCID mice also via a lateral tail vein could result in multiple metastatic tumor nodules growth in lungs as shown in Fig. 17 and Fig. 18 respectively.

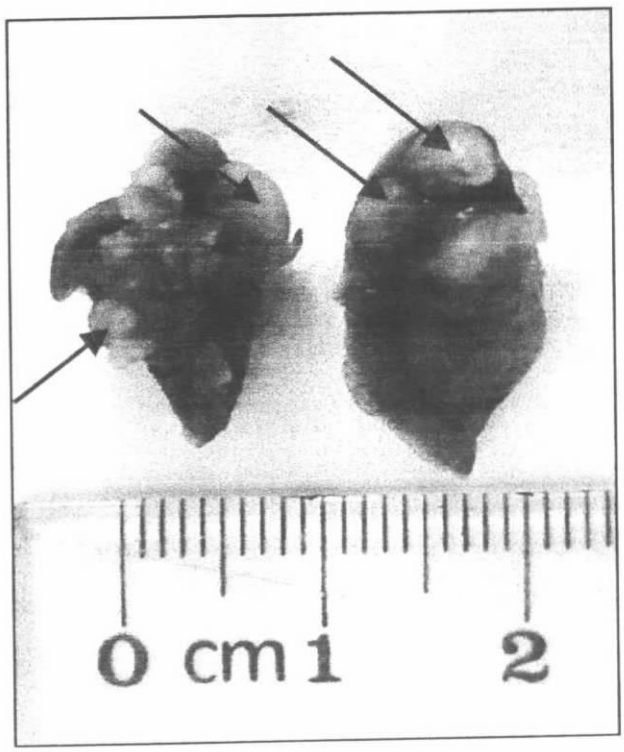

Fig. 17. Extensive tumor nodules growth indicated by arrows were observed on the lung surface of a nude mouse after i.v. injection of 3.5 x 10^6 SKOV3 tumor cells by 4 weeks.

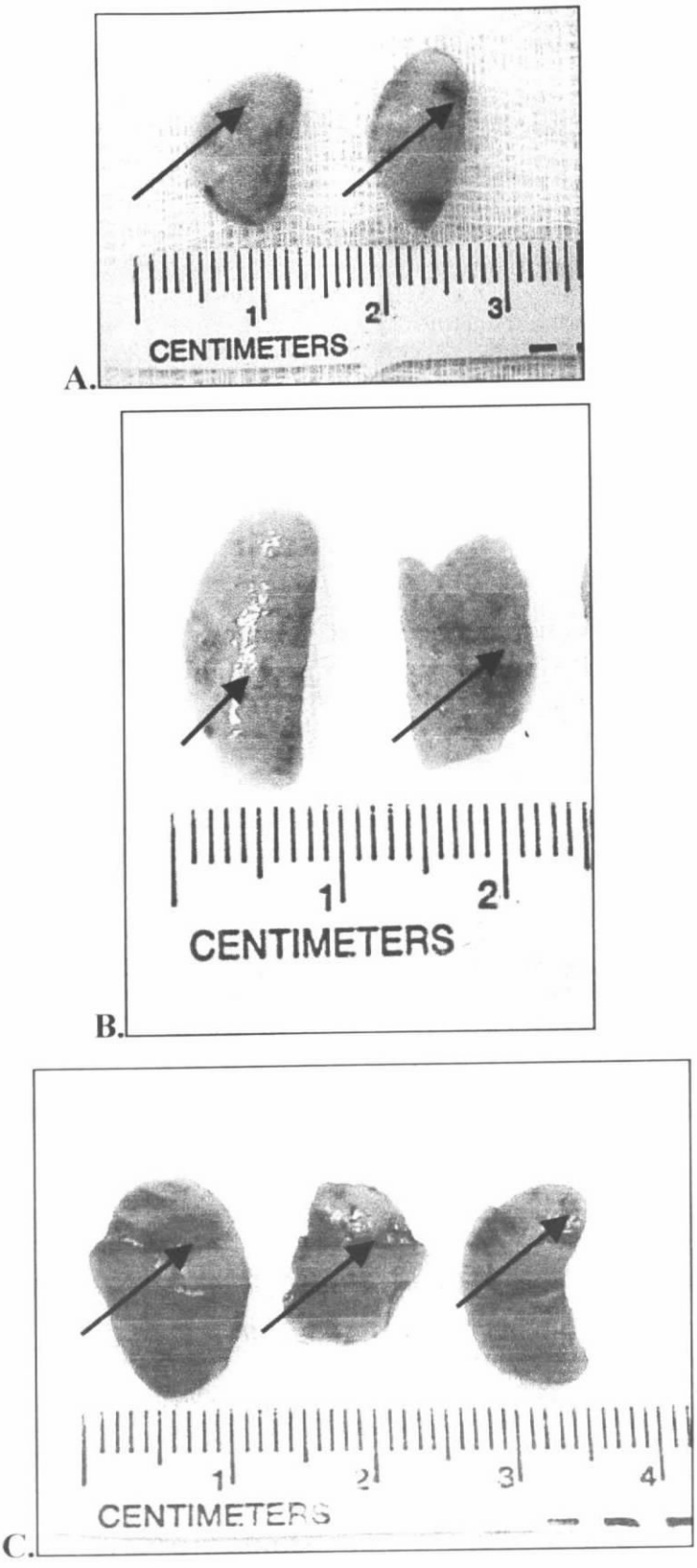

Fig. 18. Micro-metastases were observed within the lungs of SCID mice after i.v. injection of 4.8 x 10^6 (panel A), 6 x 10^6 (panel B) or 8 x 10^6 (panel C) SKOV3 tumor cells by 4 weeks as indicated by arrows.

4.5 Therapeutic Efficacy of the H520C9sFv-rhIL-2 Against "Established" Subcutaneous Tumor in SCID Mice

The therapeutic effect of the H520C9sFv-rhIL-2 on "established" subcutaneous ovarian carcinoma was tested by treating SCID mice 4 days after SKOV3 tumor cell inoculation with conditioned media from human embryonic kidney 293 cells transfected with H520C9sFv-rhIL-2 cDNA and human peripheral blood mononuclear (PBM) cells. As shown in Fig.19, objective response could be observed in one of the 2 SCID mice each treated with a daily dose of 2 μg of H520C9sFv-rhIL-2 and 5 x 10^6 human PBM cells over a period of 7 days. In contrast, the SCID mice treated with either saline alone or an equivalent mixture of saline and human PBM cells demonstrated less inhibition effect on subcutaneous tumor growth. Macroscopic observation of the subcutaneous ovarian carcinoma in the 3 treatment groups is shown in Fig.20.

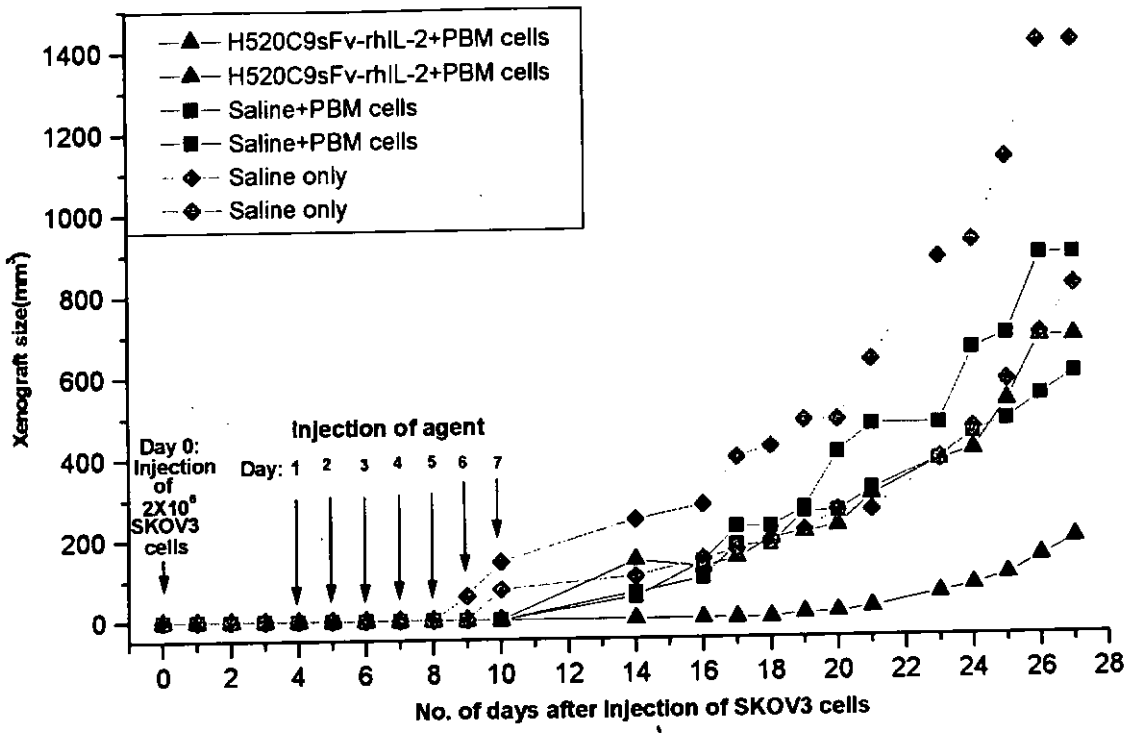

Fig. 19. Growth inhibition effect of the H520C9sFv-rhIL-2 on subcutaneous ovarian carcinoma in SCID mice. Subcutaneous ovarian carcinoma was induced by injection of 2 x 10^6 SKOV3 cells into the flank of each of 6 SCID mice. From day 4 to day 10, a daily subcutaneous injection near the original tumor cell injection site of 2 μg H520C9sFv-hIL-2 and 5 x 10^6 human PBM cells, saline with 5 x 10^6 human PBM cells, or saline alone were given to each animal. Each curve represents the daily variation of tumor size in each animal.

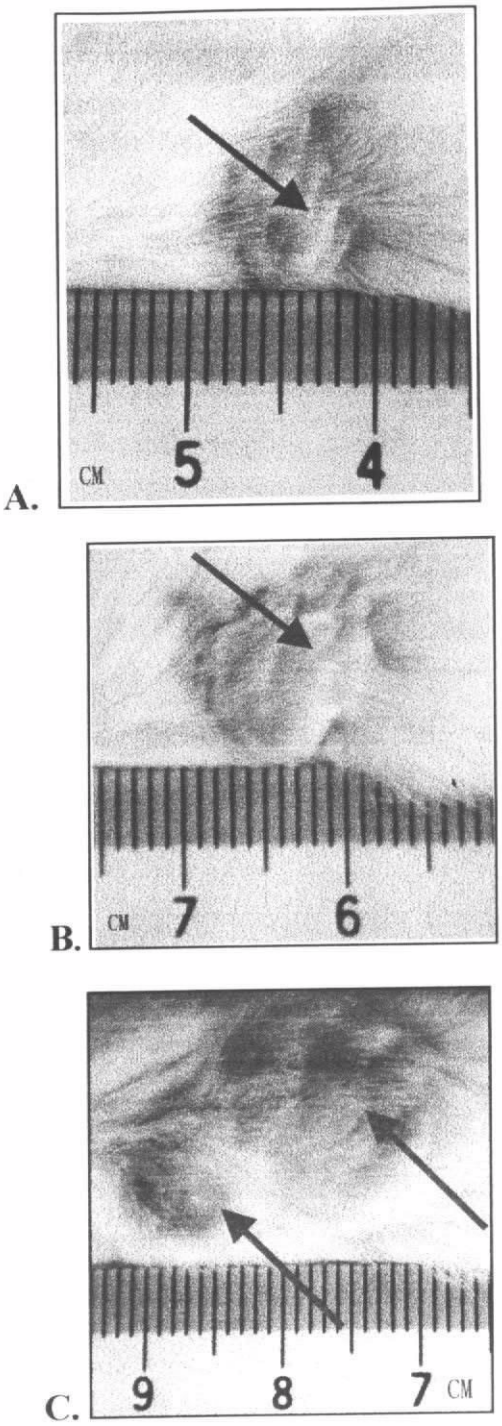

Fig. 20. Macroscopic appearance of subcutaneous ovarian SKOV3 carcinoma as indicated by arrows in SCID mice 28 days after tumor cell inoculation. 7 days treatment with daily doses of 2 μg of H520C9sFv-rhIL-2 and 5 x 10^6 human PBM cells (panel A), saline and 5 x 10^6 human PBM cells (panel B), or saline only (panel C) resulted in different objective responses of tumor growth inhibition.

4.6 Therapeutic Efficacy of the H520C9sFv-rhIL-2 Against Lung Metastases in SCID Mice

To evaluate the therapeutic effect of the H520C9sFv-rhIL-2 on human HER-2/*neu* positive ovarian metastases *in vivo*, 2 treatment experiments have been performed. The first set of treatment experiment addressed the therapeutic effect of the H520C9sFv-rhIL-2 together with human PBM cells on microscopic lung metastases in SCID mice. The lung metastases were initiated by intravenous injections of 8 x 10^6 SKOV3 tumor cells on day 0 into the animals and treatment was initiated on day 4 with daily i.v. administrations into each animal of 0.2 ml of saline, 0.2 x 10^6 PBM cells in saline, 6 μg H520C9sFv-rhIL-2, or 6 μg H520C9sFv-rhIL-2 and 0.2 x 10^6 PBM cells for 3 consecutive days. The animals were sacrificed on day 28. The results as shown in Fig. 21 and Table 1 indicate that treatment of the SCID mice with i.v. administration of a mixture of 6 μg H520C9sFv-rhIL-2 and 0.2 x 10^6 human PBM cells completely inhibited the growth of lung metastases in the SCID mice (n = 4). In contrast, the SCID mice receiving 6 μg H520C9sFv-rhIL-2 (n = 4), 0.2 x 10^6 human PBM cells (n = 4), or 0.2 ml of saline (n = 4) were ineffective in suppressing establishment of lung metastases.

	Indian ink staining on metastatic foci covering lungs surface	Magnified field of view of red squares
Group A 6 μg H520C9sFv-rhIL-2 + 0.2 x 10^6 human PBM cells.	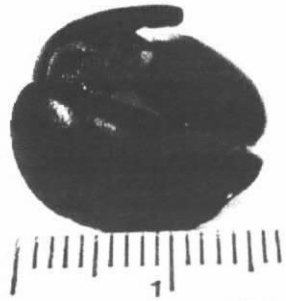	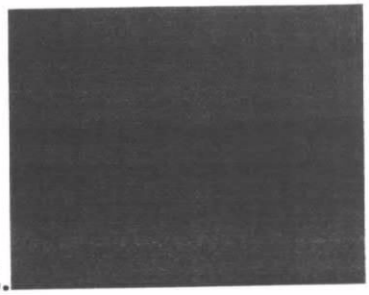
Group B 6 μg H520C9sFv-rhIL-2 only.		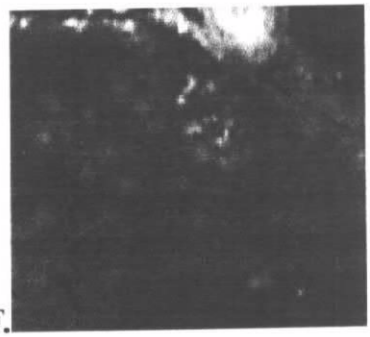
Group C 0.2 x 10^6 human PBM cells only.		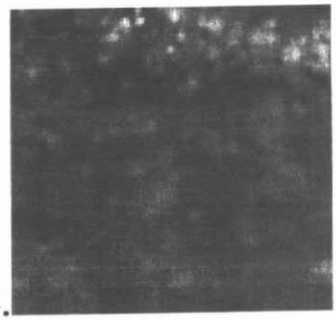
Group D Saline only.		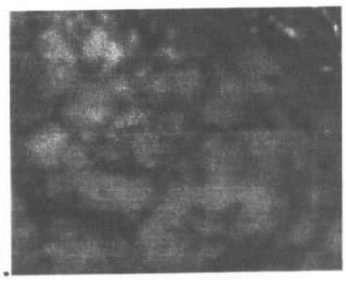

Fig. 21. Indian ink staining for evaluation of metastactic tumor growth after treatment with H520C9sFv-rhIL-2 and human PBM cells. SCID mice injected intravenously with 8 x 10^6 SKOV3 tumor cells each were allowed to grow for 4 days. They then received 3 daily treatments with 6 μg H520C9sFv-rhIL-2 and 0.2 x 10^6 PBM cells (panel A, E), 6 μg H520C9sFv-rhIL-2 only (panel B, F), 0.2 x 10^6 PBM cells only (panel C, G) or saline only (panel D, H). The mice were sacrificed on day 28. Arrows indicate positive staining of metastatic tumor foci on lungs surface of SCID mice as indicated in a magnified field of view.

Treatment	Percentage of lung surface area of SCID mice covered by metastatic foci	Mean ± Standard deviation
Group A (6 μg H520C9sFv-rhIL-2 + 0.2 x 10^6 human PBM cells)	0.4%, 0.6%, 0.8%, 1.1%	0.7 ± 0.3
Group B (6 μg H520C9sFv-rhIL-2 only)	13%, 14.8%, 18.2%, 22.3%	17.1 ± 4.1
Group C (0.2 x 10^6 human PBM cells only)	16%, 17.1%, 18%, 19.1%	17.7 ± 1.6
Group D (0.2 ml saline only)	23.9%, 27.5%, 29%, 31%	27.9 ± 2.9

Table 1. The effect of the H520C9sFv-rhIL-2 on growth of experimental lung metastases in SCID mice in terms of percentage of lung surface area covered by metastatic foci. The percentage of lung surface area covered by metastatic foci in each mouse was determined by OPTIMAS 6.0™ image analysis software.

The differences in the measured percentage of lung surface area covered by metastatic foci among the four groups of SCID mice as indicated in appendix 4 were statistically significant ($p<0.05$, One-way ANOVA). Furthermore, there was significant difference ($p<0.05$, post hoc Scheffe test) between the group mean of A and that of B, C or D. However, there was no significant difference between group B and group C.

Fig. 22 shows the means and standard deviations in the % of lung surface area covered by metastases for the 4 groups of mice.

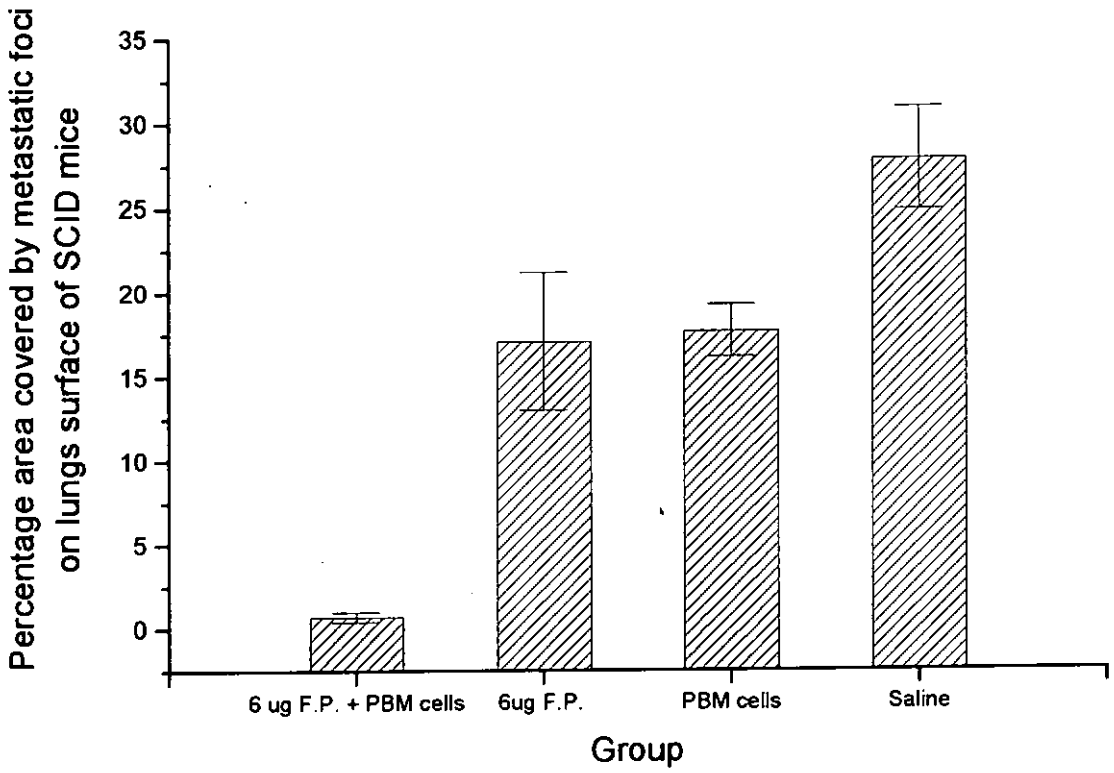

Fig. 22. Therapeutic effect of the H520C9sFv-rhIL-2 and human PBM cells on the growth of lung metastases in SCID mice. Lung metastases were induced by intravenous injections of 8 x 10^6 SKOV3 tumor cells on day 0 in SCID mice. Treatment was initiated on day 4 and consisted of daily i.v. administrations of 0.2 ml of saline, 0.2 x 10^6 PBM cells in saline, 6 μg H520C9sFv-rhIL-2, or 6 μg H520C9sFv-rhIL-2 and 0.2 x 10^6 PBM cells, for 3 consecutive days. The percentage of lung surface area covered by metastatic foci in each mouse was determined by OPTIMAS 6.0™ image analysis software. The error bars show ± one standard deviation.

The effective inhibition of lung metastases in SCID mice with treatment of H520C9sFv-rhIL-2 and human PBM cells were also evaluated by haematoxylin & eosin staining and HER-2/*neu* protein staining of lung sections removed from the mice as shown in Fig. 23. The histological and immunohistochemical staining results indicated the absence of metastatic tumor nodules within the lung sections of mice treated with a mixture of 6 μg H520C9sFv-rhIL-2 and 0.2 x 10^6 human PBM cells. In contrast, all the SCID mice treated with 6 μg H520C9sFv-rhIL-2, 0.2 x 10^6 human PBM cells, or 0.2 ml of saline showed positive staining of lung metastases.

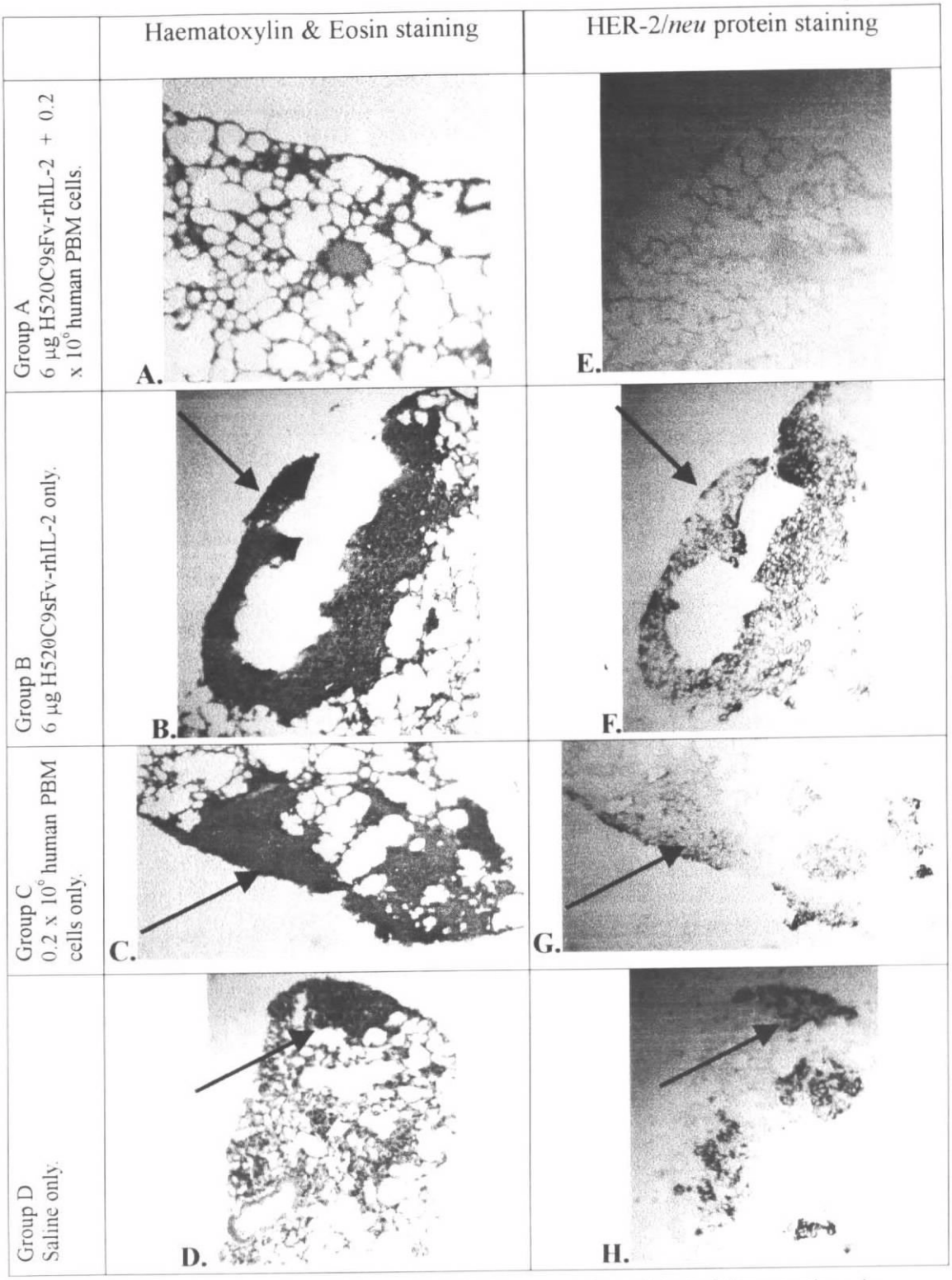

Fig. 23. Haematoxylin & eosin staining and HER-2/*neu* protein staining of lung sections in evaluation of metastactic tumor growth in SCID mice after treatment with H520C9sFv-rhIL-2 and human PBM cells. SCID mice injected intravenously with 8 x 10^6 SKOV3 tumor cells each were allowed to grow for 4 days before 3 daily treatments with 6 μg H520C9sFv-rhIL-2 and 0.2 x 10^6 PBM cells (panel A, E), 6 μg H520C9sFv-rhIL-2 only (panel B, F), 0.2 x 10^6 PBM cells only (panel C, G) or saline only (panel D, H) were given. The mice were sacrificed on day 28. Arrows indicated positive staining of metastatic tumor cells in both haematoxylin & eosin staining and HER-2/*neu* protein staining. Representative areas were photographed at a magnification of x 100.

To establish an optimal dose of H520C9sFv-rhIL-2, a second set of treatment experiment was performed. 4 days after intravenous injections of 8 x 10^6 SKOV3 tumor cells on day 0 into SCID mice, 3 daily doses of a mixture of 3 μg H520C9sFv-rhIL-2 and 0.2 x 10^6 human PBM cells, 6 μg H520C9sFv-rhIL-2 and 0.2 x 10^6 human PBM cells or saline alone were administered intravenously into each animal. The mice were sacrificed 28 days later. Indian ink staining of the lungs of the mice was performed (Fig. 24). Table 2 shows the differences in measured percentage of lung surface area covered by metastatic foci for the 3 treatment groups of mice. Treatment with 6 μg H520C9sFv-rhIL-2 and 0.2 x 10^6 human PBM cells completely inhibited growth of lung metastases in SCID mice. In contrast, the other two groups were ineffective in this regard. The differences in the measured percentage of lung surface area covered by metastatic foci among the three groups of SCID mice as indicated in appendix 5 were statistically significant ($p<0.05$, One-way ANOVA).

Treatment	Indian ink staining on metastatic foci covering lung surface	Magnified field of view of red squares
Group A 6 μg H520C9sFv-rhIL-2 + 0.2 x 10^6 human PBM cells.	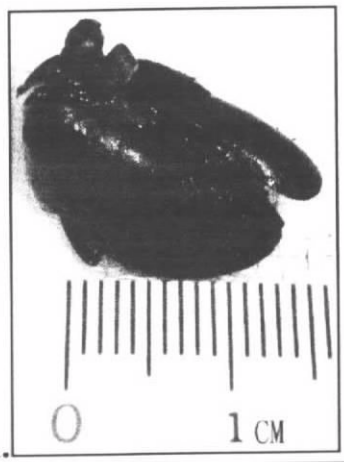 A.	D. 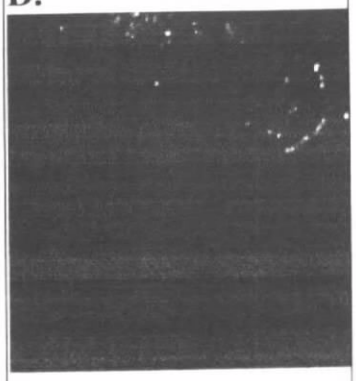
Group B 3 μg H520C9sFv-rhIL-2 + 0.2 x 10^6 human PBM cells.	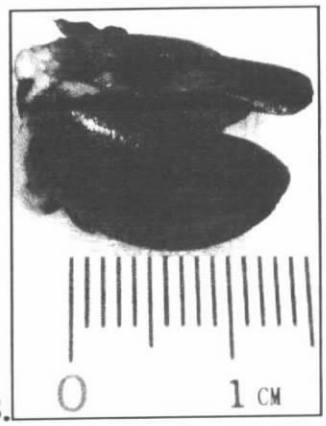 B.	E. 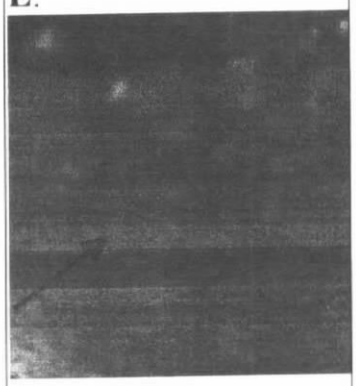
Group C Saline only.	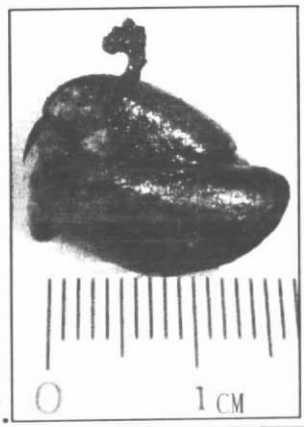 C.	F. 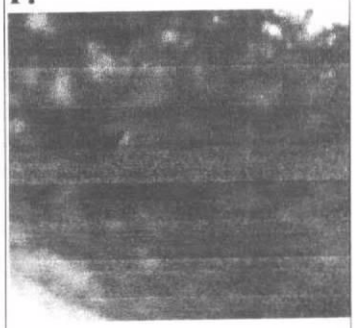

Fig. 24. Indian ink staining for evaluation of metastactic tumor growth in SCID mice after different combined doses of treatment with the H520C9sFv-rhIL-2 and human PBM cells. SCID mice injected intravenously with 8 x 10^6 SKOV3 tumor cells each were allowed to grow for 4 days. They then received 3 daily treatments with 6 μg H520C9sFv-rhIL-2 and 0.2 x 10^6 PBM cells (panel A, D), 3 μg H520C9sFv-rhIL-2 and 0.2 x 10^6 PBM cells (panel B, E), or saline (panel C, F). The mice were sacrificed on day 28. Arrows indicate positive staining of metastatic tumor foci on lungs surface of SCID mice as indicated in a magnified field of view.

Treatment	Percentage of lung surface area of SCID mice covered by metastatic foci	Mean ± Standard deviation
Group A (6 μg H520C9sFv-rhIL-2 + 0.2 x 10^6 human PBM cells)	0.1%, 0.1%, 0.2%, 0.5%	0.2 ± 0.2
Group B (3 μg H520C9sFv-rhIL-2 + 0.2 x 10^6 human PBM cells)	16.6%, 25.5%, 26.9%, 29.8%	24.7± 5.7
Group C (0.2 ml saline only)	20.7%, 24.7%, 34.7%, 36.6%	29.2 ± 7.7

Table 2. The effect of different doses of the H520C9sFv-rhIL-2 with human PBM cells on experimental lung metastases in SCID mice. The percentage of lung surface area of SCID mice covered by metastatic foci was counted by OPTIMAS 6.0™ image analysis software.

As shown in appendix 5, differences between group A and the other 2 groups in terms of measured percentage of lung surface area covered by metastatic foci were statistically significant ($p< 0.05$, post hoc Scheffe test). However, there was no significant difference between treatment group B and treatment group C. The group means and standard deviations of percentage area covered for various treatment groups are shown in Fig. 25.

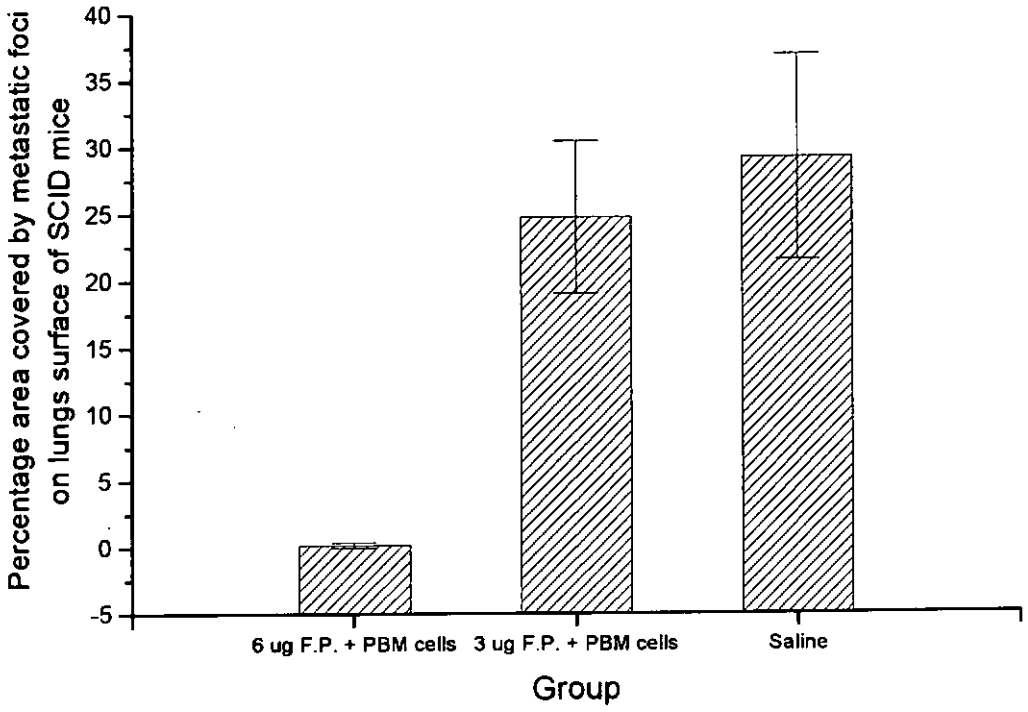

Fig. 25. Therapeutic effect of different doses of the H520C9sFv-rhIL-2 and human PBM cells on the establishment of lung metastases in SCID mice. Lung metastases were induced by intravenous injections of 8 x 10^6 SKOV3 tumor cells on day 0 in SCID mice. Treatment was initiated on day 4 and consisted of daily i.v. administrations of 6 μg H520C9sFv-rhIL-2 and 0.2 x 10^6 PBM cells, 3 μg H520C9sFv-rhIL-2 and 0.2 x 10^6 PBM cells, or 0.2 ml saline as indicated for 3 consecutive days. The percentage of lung surface area covered by metastatic foci in each mouse was determined by OPTIMAS 6.0™ image analysis software. The error bars show ± one standard deviation.

As shown in Fig. 26, the histological haematoxylin & eosin staining results indicated treatment of SCID mice in group A with a mixture of 6 μg H520C9sFv-rhIL-2 and 0.2 x 10^6 human PBM cells effectively inhibited the growth of lung metastases in SCID because of the absence of tumor nodules within lung sections. In contrast, the other groups of SCID mice had positive staining of tumor nodules within some lung sections.

Treatment	Haematoxylin & Eosin staining
Group A 6 μg H520C9sFv-rhIL-2 + 0.2 x 10^6 human PBM cells.	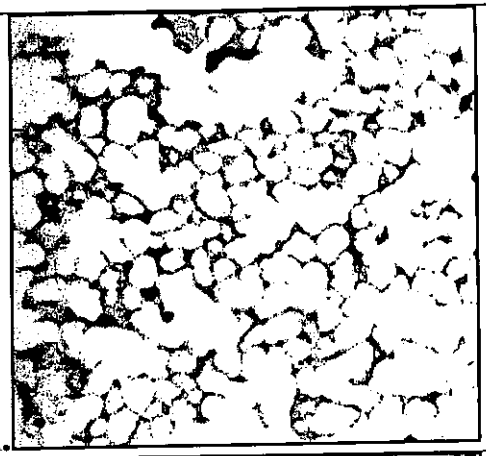 A.
Group B 3 μg H520C9sFv-rhIL-2 + 0.2 x 10^6 human PBM cells	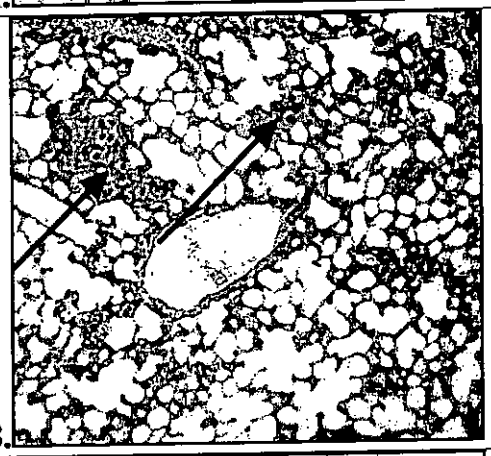 B.
Group C 0.2 ml saline only.	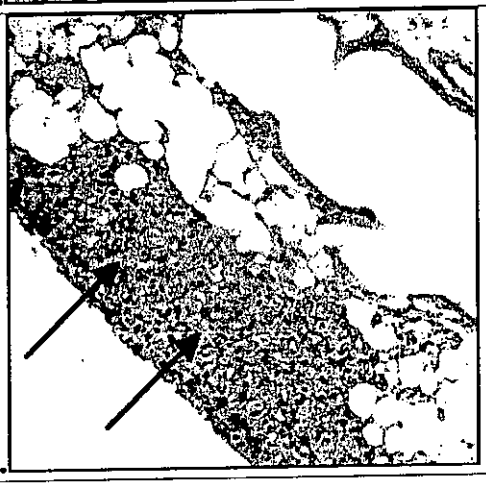 C.

Fig. 26. Haematoxylin & eosin staining in evaluation of metastactic tumor growth in lung sections of SCID mice after different combined doses of H520C9sFv-rhIL-2 and human PBM cells treatment. SCID mice injected intravenously with 8 x 10^6 SKOV3 tumor cells each were allowed to grow for 4 days before 3 daily treatments with 6 μg H520C9sFv-rhIL-2 and 0.2 x 10^6 PBM cells (panel A), 3 μg H520C9sFv-rhIL-2 and 0.2 x 10^6 PBM cells (panel B), or 0.2 ml saline only (panel C) were given. The mice were sacrificed on day 28. Arrows indicated positive staining of metastatic tumor cells. Representative areas were photographed at a magnification of x 100.

Chapter 5

Discussion

5.1 Characterization of the H520C9sFv-rhIL-2

This study demonstrated that a recombinant antibody-cytokine fusion protein, H520C9sFv-rhIL-2, consisting of a humanized single chain antibody and recombinant human IL-2 retained both antibody and IL-2 functions. The results of SDS-PAGE and Western blot analysis in Fig. 2 confirmed the results of an earlier report (Li et al, 1999) that the H520C9sFv-rhIL-2 had a molecular weight of about 45 kDa and consisted of one IL-2. The purified H520C9sFv-rhIL-2 was shown in Fig.3 to retain the binding specificity against human HER-2/*neu* proto-oncogene product, p185, of the parental 520C9 mAb in a cellular ELISA on human SKOV3 cells but did not bind to HeLa cells without p185 expression. In a positive control cellular ELISA, 520C9 was shown to bind to SKOV3 cells, but not to p185 negative HeLa cells.

5.2 Development of Animal Tumor Models using SKOV3 Tumor Cells

Different experimental tumor models were successfully developed using SKOV3 ovarian tumor cells in both nude and SCID mice. Firstly, subcutaneous injections of 3 different SKOV3 cell numbers have been applied to 3 nude mice respectively in order to observe growth of subcutaneous xenograft (Fig. 7). A subcutaneous injection of 2.5×10^6 SKOV3 tumor cells in 0.2ml RPMI 1640 at the flank of a nude mouse was capable to establish a subcutaneous tumor nodule of about 500 mm^3 1 month post tumor cell inoculation as shown in Fig. 8. In addition, the subcutaneous tumor nodule developed a blood vessel network for its active growth and severe necrosis (Fig. 10). The nude mouse injected with 10×10^6 SKOV3 tumor cells could only tolerate the subcutaneous tumor load for 26 days and the mouse died from severe necrosis of the tumor nodule. On the other hand, the nude mouse injected with 5×10^6 SKOV3 tumor cells subcutaneously could survive for 36 days with tumor load. Although the subcutaneous growth of SKOV3 tumor cells in SCID mice did not determine in this study, similar subcutaneous tumor growth kinetics were assumed in

both nude and SCID mice.

Secondly, injection of 6 x 10^6 SKOV3 tumor cells into the peritoneum of a nude mouse resulted in severe bloody ascites and peritoneal dissemination of tumor nodules within the mesenterium 3 weeks later (Fig. 13). In addition, an invasive growth of SKOV3 tumor cells into the liver capsule was also observed in another nude mouse 3 weeks after intraperitoneal injection of 8 x 10^6 SKOV3 tumor cells (Fig. 15). SCID mice were also employed to develop intraperitoneal tumors using SKOV3 tumor cells. SKOV3 tumor nodules were observed within the mesenterium 2 weeks after intraperitoneal injection of 3 x 10^6 or 6 x 10^6 SKOV3 tumor cells as shown in Fig. 16.

Several researchers have established animal tumor models for testing the therapeutic efficacy of antibody-IL-2 fusion proteins against human malignancies. The effective eradication of experimental disseminated lung metastases in animals with recombinant antibody-IL-2 fusion proteins were mentioned by Xiang et al (1997) and Dolman et al (1998) in syngeneic BALB/C mice with colon carcinoma and in SCID mice with prostate carcinoma respectively using

hukS1/4-IL-2 fusion protein as well as Becker et al (1999) in C57 BL/6 mice with melanoma using ch14.18-IL-2 fusion protein. The induction of experimental lung metastases was induced by intravenous injection of carcinoma cells via the lateral tail veins of mice. Grossly visible metastases were detectable on the surface of the lungs 28 days after tumor cell injections. On the other hand, complicated experimental hepatic metastases could also be successfully developed in Lode et al (1998) and Sabzevari et al (1994) by intra-splenic injection of carcinoma cells followed by ligation of the splenic pedicle with 4.0 silk suture and then removal of the spleen 2 min. later. Disseminated metastases were observed throughout the liver tissues 4 days after tumor cells injection.

In order to evaluate the therapeutic potential of the H520C9sFv-rhIL-2 against HER-2/*neu* positive metastases in this study, metastatic lung tumors have been successfully developed after intravenous injections of appropriate numbers of SKOV3 cells into nude mice or SCID mice. 4 weeks after an intravenous injection of 6 x 10^6 SKOV3 tumor cells into a nude mouse via a lateral tail vein, multiple tumor nodules were grown on the lung surface (Fig. 17). However, micro-metastases of

SKOV3 tumor were noticed within the lungs of SCID mice 4 weeks after intravenous injections of 4.8 x 10^6 SKOV3 cells as shown in Fig. 18. These results in immunodeficient mice provide opportunities to assess the therapeutic properties of the H520C9sFv-rhIL-2.

5.3 Antitumor Responses induced by the H520C9sFv-rhIL-2

Antitumor responses induced by the H520C9sFv-rhIL-2 against human HER-2/*neu* positive ovarian carcinoma were assessed in 2 different experimental treatment models. Firstly, treatment effect in term of growth inhibition of subcutaneous SKOV3 tumor xenograft in SCID mice was determined in the presence and absence of H520C9sFv-rhIL-2 and human PBM cells as shown in Fig.19. It was observed that treatment with a daily dose of 2 μg H520C9sFv-rhIL-2 and 5 x 10^6 human PBM cells over a period of 7 days slowed down the growth of subcutaneous xenograft in one SCID mouse. In contrast, saline and equal number of human PBM cells alone demonstrated less inhibition effect on subcutaneous tumor growth in other mice.

Secondly, the therapeutic effect of the H520C9sFv-rhIL-2 in term of inhibition of lung metastases development in SCID mice was assessed. Treatment of SCID mice 4 days after intravenous tumor cell inoculation by intravenous administration of 6 μg H520C9sFv-rhIL-2 and 0.2 x 10^6 human PBM cells on 3 consecutive days was able to completely inhibit the growth of lung metastases. The complete inhibition was confirmed by means of histological Haematoxylin & Eosin staining and immunohistochemical staining for HER-2/*neu* p185 protein on consecutive sections of lung specimens (Fig. 23). In contrast, neither the treatment of SCID mice with 0.2 x 10^6 human PBM cells nor 6 μg H520C9sFv-rhIL-2 alone in the same treatment schedule had a complete inhibition on the growth of lung metastases. In another treatment experiment, the daily injection of 3 μg H520C9sFv-rhIL-2 and 0.2 x 10^6 human PBM cells on 3 consecutive days was unable to completely inhibit the growth of lung metastases in the same metastatic model of SCID mice (Fig. 26). The induction of an anti-tumor response by the H520C9sFv-rhIL-2 and human PBM cells explained the observed therapeutic effect against establishment of subcutaneous tumors and lung metastases. Since the employed SCID mice in this study are deficient in NK cells, T cells and B cells, the

therapeutic responses are most likely due to the stimulation of the injected human PBM cells by the H520C9sFv-rhIL-2 fusion protein.

IL-2 exhibits a wide variety of biological activities, including the stimulation of antitumor effector cells such as cytotoxic T cells, NK cells and macrophages (Whittington, 1993). Mass et al in 1993 reported that stimulation of human peripheral blood mononuclear cells by IL-2 generated unique activated lymphocyte populations of largely NK cell phenotype. They are called lymphokine-activated killer (LAK) cells which effectively mediated anti-tumor response. The ability of the H520C9sFv-rhIL-2 to support the proliferative activity of the IL-2-dependent cell line, CTLL-2, and to generate LAK cells in vitro was reported by Li et al (1999). The results clearly demonstrated that there was no significant loss of bioactivity of the IL-2 moiety of the fusion protein. In addition, LAK cells generated by the IL-2 moiety of the H520C9sFv-rhIL-2 demonstrated similar effect in the killing of target Daudi cells when compared to LAK cells activated by rhIL-2 in the cytotoxicity assay. The mechanism responsible for the observed antitumor activities of the H520C9sFv-rhIL-2 together with human PBM cells in SCID mice is not known, but may be mediated through

human LAK cells. Lode et al (2000), Reisfeld and Gillies (1996) and Gillies et al (1992) have extensively analyzed the therapeutic effect of antibody-IL-2 fusion protein between IL-2 and the chimeric anti-GD2 ganglioside antibody (ch14.18) that recognizes the colon carcinoma-associated antigen in syngeneic mouse models. This result demonstrated that the fusion proteins were effective in eradicating established experimental metastatic tumors through the activation of $CD8^+$ T lymphocytes and NK cells. In this study, once the H520C9sFv-rhIL-2 was targeted into the HER-2/*neu* overexpressed tumor environment, the IL-2 moiety might activate and expand a variety of immune effector cells, including T lymphocytes, NK cells, macrophages or granulocytes against the injected tumor cells. This may also explain why partial inhibition of lung metastatic growth was observed in SCID mice treated with the fusion protein alone (Fig. 22) because SCID mice have functional macrophages and granulocytes.

5.4 Limitations and Recommendations of the Study

There were several limitations of this study. Firstly, although the intraperitoneal SKOV3 tumor models in nude and SCID mice were successfully established, due to limited time of this study, the therapeutic potential of the H520C9sFv-rhIL-2 against SKOV3 tumor in the intraperitoneal tumor models has not yet been determined. Further treatment experiments using these models should be performed.

Secondly, in the treatment experiments to evaluate the therapeutic efficiency of the H520C9sFv-rhIL-2 against the growth of subcutaneous tumors in SCID mice, the sample size of the animals used was small due to limited time of study. It is better to have a larger sample size in each group of animal for meaningful statistical analysis. At least 4 SCID mice in each group are required to give more convincing and reliable result.

Thirdly, further studies are anticipated to explore the effector cells responsible for the antitumor responses of the H520C9sFv-rhIL-2 in

tumor bearing mice. Immunophenotyping of the involved effector cells, such as $CD8^+$ T lymphocytes, $CD4^+$ T lymphocytes and NK cells, present in the treated lungs should be performed. In addition, the existence of 30 kDa band in the Western blot in Fig. 2 indicated a fragment of the fusion protein containing IL-2 or an IL-2 dimer. Further comparison treatment experiments should be performed, such as IL-2 with or without PBMCs, functional or mutant H520C9sFv-rhIL-2 fusion protein with PBMCs, in SCID mice bearing both HER-2/*neu* positive (SKOV3) and HER-2/*neu* negative (HeLa) tumor. These comparison experiments can prove whether the 30kDa band unknown protein may contribute to some, unlikely all, of the observed therapeutic effect.

Fourthly, further studies are warranted in optimizing the treatment protocol such as the schedule, route and optimal doses of adminstration of the H520C9sFv-rhIL-2. Although no metastatic tumor foci were detected by macroscopic Indian ink staining and histological examination on lung sections stained with Haematoxylin & Eosin or anti-HER-2/neu antibody for those SCID mice treated with 6 μg H520C9sFv-rhIL-2 and 2 x 10^5 human PBM cells, it is still

possible that the mice could carry minimal residual disease. To rule out this possibility, the treated animals should be followed for longer periods of time to see if there is any relapse.

Chapter 6

Conclusion

In conclusion, the present research study demonstrated that a recombinant antibody-cytokine fusion protein, H520C9sFv-rhIL-2, was expressed stably in transfected 293 cells and retained both the binding specificity against human SKOV3 cells overexpressing HER-2/*neu* and IL-2 activity. The ability of the H520C9sFv-rhIL-2 to induce a cellular immune response that suppressed the growth of subcutaneous xenograft and lung metastases of SKOV3 in SCID mice was investigated. Although the mechanisms of tumor cell killing induced by the H520C9sFv-rhIL-2 is not yet determined in this study, the likely effector cells are human T cells, NK cells, macrophages and granulocytes. These pre-clinical findings suggested that the H520C9sFv-rhIL-2 might provide an effective way of targeting effective doses of IL-2 to tumors with HER-2/*neu* overexpression without increasing systemic toxicity. This approach may offer a new adjuvant immunotherapy for patients with HER-2/*neu* positive metastatic cancers.

Chapter 7

References

1 Baars, J.W., Hack, C.E., Wagstaff, J., Eerenberg-Belmer, A.J.M., Wolbink, G.J., Thijs, L.G., Strack van Schijndel, R.J.M., Van del Vall, H.L.J.A., and Pinedo, H.M. "The activation of polymorphonuclear neutrophils and the complement system during immunotherapy with recombinant Interleukin-2". *Br. J. Cancer*, Vol. 65, pp. 96-101 (1992)

2 Becker, J.C., Pancook, J.D., Gillies, S.D. and Furukawa, K. and Reisfeld, R.A. "T-cell mediated eradication of murine metastatic melanoma induced by targeted interleukin 2 therapy". *J. Exp. Med.*, Vol. 183, pp.2361-2366 (1996)

3 Becker, J.C., Pancook, J.D., Gillies, S.D., Mendelsohn, J. and Reisfeld, R.A. "Eradication of human hepatic and pulmonary melanoma metastases in SCID mice by antibody-interleukin 2 fusion proteins". *Proc. Natl. Acad. Sci. USA,* Vol. 93, pp.2702-2707 (1999)

4 Becker, J.C., Varki, N., Gillies, S.D., Furukawa, K. and Reisfeld, R.A. "Long-lived and transferable tumor immunity in mice after targeted interleukin-2 therapy". *J. Clin. Invest.*, Vol. 98, pp.2801-2804 (1996)

5 Becker, J.C., Varki, N., Gillies, S.D., Furukawa, K. and Reisfeld, R.A. "An antibody-interleukin 2 fusion protein overcomes tumor heterogeneity by induction of a cellular immune response". *Proc. Natl. Acad. Sci. USA,* Vol. 93, pp.7826-7831 (1996)

6 Carter, P., Presta, L., Gorman, C.M., Ridgway, J.B.B., Henner, D., Wong, W.L.T., Rowland, A.M., Kotts, C., Carver, M.E. and Shepard, H.M. "Humanization of an p185^{HER-2} antibody for human cancer therapy". *Proc. Natl. Acad. Sci. USA*, Vol. 89, pp.4285-4289 (1992)

7 Cirisano, F.D. and Karlan, B.Y. "The role of the HER-2/*neu* oncogene in gynecologic cancers. *J. Soc.Gynecol Investig*, Vol. 3, pp.99-105 (1996)

8 Dillman, R.O. "What to do with IL-2 ?". *Cancer Biotherapy and Radiopharmaceuticals*, Vol.14, pp.423-434 (1999).

9 Dolman, C.S., Mueller, B.M., Lode, H.N., Xiang, R., Gillies, S.D. and Reisfeld, R.A. "Suppression of human prostate carcinoma metastases in severe combined immunodeficient mice by interleukin-2 immunocytokine therapy". *Clinical Cancer Research*, Vol. 4, pp.2552-2557 (1998)

10 Donohue, J.H. and Rosenberg S.A. "The fate of interleukin-2 after *in vivo* administration". *The Journal of Immunology*, Vol. 130, pp.2203-2208 (1983)

11 Fendly, B.M., Kotts, C., Vetterlein, D., Lewis, G.D., Winget, M., Carver, M.E., Watson, S.R., Sarup, J., Saks, S., Ullrich, A. and Shepard, H.M. "The extracellular domain of HER2/*neu* is a potential immunogen for active specific immunotherapy of breast cancer". *Journal of Biological Response Modifiers*, Vol. 9, pp.449-455 (1990)

12 Gillies, S.D., Reilly, E.B., Lo, K.M. and Reisfeld, R.A. "Antibody-targeted interleukin 2 stimulates T-cell killing of autologous tumor cells", *Proc. Natl. Acad. Sci. USA*, Vol. 89, pp.1428-1432 (1992)

13 Hornick, J. L., Khawli, L. A., Hu, P. S., Sharifi, J., Khanna, C., and Epstein, A. L. "Pretreatment with a monoclonal antibody/interleukin-2 fusion protein directed against DNA enhances the delivery of therapeutic molecules to solid tumors". *Clinical Cancer Research*, Vol. 5, pp.51-60, (1999)

14 Hung, M.C. and Lau, Y.K. "Basic science of HER-2/*neu*: a review". *Semin. Oncol.*, Vol. 26, pp.51-59 (1999)

15 Kwok, C.S., Cheung, W.K., Yip, T.C., Lau, W.H., Newberry, R.A. and Austin, R.C. "A novel vasoactive human interleukin-2/single chain antibody fusion protein for HER-2 positive tumors". *Proceedings of the 92nd American Association of Cancer Research*, New Orleans, LA, 24-28 March, 2001, pp. 290-291 (2001)

16 Lafreniere, R. and Rosenberg, S.A. "Successful imunotherapy of murine experimental hepatic metastases with lymphokine-activated killer cells and recombinant interleukin 2". *Cancer Research*, Vol. 45, pp.3735-3741 (1985)

17 Li, J., Gyorffy, S. F., Ring, D. B., Kwok, C. S., and Austin, R. C. "Preparation and characterization of a recombinant humanized single-chain Fv antibody/human interleukin-2 fusion protein directed against the HER-2/*neu* (c-erbB2) proto-oncogene product, p185". *Tumor Targeting*, Vol. 4, pp.105-114 (1999)

18 Lode, H.N., Xiang, R., Becker, J.C., Gillies, S.D. and Reisfeld, R.A. "Immunocytokines: A promising approach to cancer immunotherapy". *Pharmacol. Ther.*,Vol. 80, pp.277-292 (1998)

19 Lode, H.N., Xiang, R., Becker, J.C., Gillies, S.D. and Reisfeld, R.A. "Amplification of T cell-mediated immune responses by antibody-cytokine fusion proteins". *Immunological Investigations*, Vol. 29, pp.117-120 (2000)

20 Lode, H. N., Xiang, R., Dreier, T., Varki, N. M., Gillies, S. D., and Reisfeld, R. A. "Natural killer cell-mediated eradication of neuroblastoma metastases to bone marrow by targeted interleukin-2 therapy". *Blood*, Vol.91, pp.1706-1715 (1998)

21 Lotze, M.T., Chang, A.E., Seipp, C.A., Simpson, C., Vetto, J.T. and Rosenberg, S.A. "High-dose recombinant interleukin-2 in the treatment of patients with disseminated Cancer – Responses, treatment-related morbidity and histologic findings". *JAMA*, Vol. 256, pp.3117-3124 (1986)

22 Maas, R.A., Dullens, F.J. and Otter, W.D. "Interleukin-2 in cancer treatment: disappointing or (still) promising? A review". *Cancer Immunol Immunother*, Vol. 36, pp.141-148 (1993)

23 Maas, R.A., Van Weering, D.H., Dullens, H.F. and Den Otter, W. "Intratumoral low-dose interleukin-2 induces rejection of distant solid tumor". *Cancer Immunol Immunother*, Vol. 33, pp.389-394 (1991)

24 Meden, H. and Kuhn, B.Y. "Overexpression of the oncogene c-erbB2 (HER2/*neu*) in ovarian cancer: a new prognostic factor". *Eur J. Obstet Gynecol Reprod Biol*, Vol. 72, pp.173-179 (1997)

25 Melani, C., Figini, M., Nicosia, D., Luison, E., Ramakrishna, V., Casorati, G., Parmiani, G., Eshhar, Z., Canevari, S., and Colombo, M. P. "Targeting of interleukin 2 to human ovarian carcinoma by fusion with a single-chain Fv of antifolate receptor antibody". *Cancer Research*, Vol.58, pp.4146-4154 (1998)

26 Oppenheim, M.H. and Lotze, M.T. "Interleukin-2: Solid-tumor therapy". *Oncology*, Vol.51, pp.154-169 (1994)

27 Pegram, M.D., Lipton, A., Hayes, D.F., Weber, B.L., Baselga, J.M., Tripathy, D., Baly, D., Baughman, S.A., Twaddell, T., Glaspy, J.A. and Slamon, D.J. "Phase II study of receptor-enhanced chemosensitivity using recombinant humanized anti-p185$^{HER2/neu}$ monoclonal antibody plus cisplatin in patients with HER2/*neu*-overexpressing metastatic breast cancer refractory to chemotherapy treatment". *Journal of Clinical Oncology*. Vol.16, pp. 2659-2671 (1998)

28 Penichet, M. L., Harvill, E. T., and Morrison, S. L. "An IgG3-IL-2 fusion protein recognizing a murine B cell lymphoma exhibits effective tumor imaging and antitumor activity". *J. Interferon Cytokine Res*, Vol.18, pp.597-607 (1998)

29 Reese, D.M. and Slamon, D.J. "HER-2/*neu* signal transduction in human breast and ovarian cancer". *Stem Cells*, Vol.15, pp.1-8 (1997)

30 Reisfeld, R.A. and Gillies, S.D. "Antibody-interleukin 2 fusion proteins: A new approach to cancer therapy". *Journal of Clinical Laboratory Analysis*, Vol. 10, pp.160-166 (1996)

31 Rosenberg, S.A., Lotze, M.T., Yang, J.C., Aebersold, P.M., Linehan, W.M., Seipp, C.A. and White, D.E. "Experience with the use of high-dose interleukin-2 in the treatment of 652 cancer patients". *Ann. Surg*, Vol. 210, pp. 474-485 (1989)

32 Rosenberg, S.A., Mule, J.J., Spiess, P.J., Reichert, C.M. and Schwarz, S.L. "Regression of established pulmonary metastases and subcutaneous tumor mediated by the systemic administration of high-dose recombinant interleukin 2". *J. Exp. Med.*, Vol.161, pp.1169-1188 (1985)

33 Riethmuller, G., Gadicke, E.S. and Johnson, J.P. "Monoclonal antibodies in cancer therapy". *Current Opinion in Immunology*, Vol. 5, pp.732-739 (1993)

34 Ring, D.B., Clark, R. and Saxena, A. "Identity of BCA200 and c-erbB-2 indicated by reactivity of monoclonal antibodies with recombinant c-erbB-2". *Molecular Immunology*, Vol. 28, pp.915-917 (1991)

35 Sabzevari, H., Gillies, S.D., Mueller, B.M., Pancook, J.D. and Reisfeld, R.A. "A recombinant antibody-interleukin 2 fusion protein suppresses growth of hepatic human neuroblastoma metastases in severe combined immunodeficiency mice". *Proc. Natl. Acad. Sci. USA*, Vol. 91 pp.9626-9630 (1994)

36 Siegel, J.P. and Puri, R.K. "Interleukin-2 Toxicity". *Journal of Clinical Oncology*, Vol.9, pp.694-704 (1991)

37 Szollosi, J., Balazs, M., Feuerstein, B.G., Benz, C.C. and Waldman, F.M. "ERBB-2 (HER-2/*neu*) gene copy number, $p185^{HER-2}$ overexpression, and intratumor heterogeneity in human breast cancer". *Cancer Research*, Vol. 55, pp.5400-5407 (1995)

38 Tandon, A.K., Clark, G.M., Chamness, G.C., Ullrich, A. and McGuire, W.L. "HER-2/*neu* oncogene protein and prognosis in breast cancer". *Journal of Clinical Oncology*, Vol. 7, pp.1120-1128 (1989)

39 Toikkanen, S., Helin, H., Isola, J. and Josensuu, H. "Prognostic significance of HER-2 oncoprotein expression in breast cancer: A 30-year follow-up ". *Journal of Clinical Oncology*, Vol. 10, pp.1044-1048 (1992)

40 Vial, T. and Descotes, J. "Clinical toxicity of interleukin-2". *Drug Safety*, Vol. 7, pp.417-433 (1992)

41 Whittington, R. and Faulds, D. "Interleukin-2 – A review of its pharmacological properties and therapeutic use in patients with cancer". *Drug Evaluation*. Vol. 46, pp. 446-514 (1993)

42 Wong, Y.F., Cheung, T.H., Lam, S.K., Lu, H.J., Zhuang, Y.L., Chan, M.Y. and Chung, T.K. "Prevalence and significance of HER-2/neu amplification in epithelial ovarian cancer". *Gynecol Obstet Invest*, Vol. 40, pp.209-212 (1995)

43 Xiang, J., Liu, E., Moyana, T. and Qi, Y. "Single-chain antibody variable region-targeted interleukin-2 stimulates T cell killing of human colorectal carcinoma cells". *Immunology and Cell Biology*, Vol. 72, pp.275-285 (1994)

44 Xiang, R., Lode, H.N., Dolman, C.S., Dreier, T., Varki, N.M., Qian, X., Lo, K.M., Lan, Y., Super, M., Gillies, S.D. and Reisfeld, R.A. "Elimination of established murine colon carcinoma metastases by antibody-interleukin 2 fusion protein therapy". *Cancer Research*, Vol. 57, pp.4948-4955 (1997)

45 Yu, D., Wolf, J.K., Scanlon, M., Price, J.E. and Hung, M.C. "Enhanced c-erbB-2/*neu* expression in human ovarian cancer cells correlates with more severe malignancy that can be suppressed by E1A". *Cancer Research*, Vol. 53, pp.891-898 (1993)

Chapter 8

APPENDICES

Appendix 1

Kwok, C.S., Yip, T.C., Cheung, W.K., Leung, K.L., So, F.F., Ma, V.M. and Lau, W.H. "Preclinical study of a novel vasoactive human interleukin-2/single chain antibody fusion protein for HER-2 positive tumors" *Proceedings of the 94th American Association of Cancer Research*, Washington, DC, 11-14 July, p.1289 (2003)

This study is a continuing pre-clinical effort to characterize a novel vasoactive fusion protein (FP) for treating HER-2 positive tumors. The FP consists of a recombinant human IL-2 and a recombinant humanized single-chain Fv (sFv) antibody which combines the V_H and V_L portions of a murine MoAb (520C9) specific for human HER-2 (Li J. et al, Preparation and characterization of a recombinant humanized single-chain Fv antibody/human interleukin-2 fusion protein directed against the HER-2/neu (c-erb B2) proto-oncogene product, p185. Tumor Targeting 4: 105-114,1999). We had previously reported preliminary experiments to characterize the anti-tumor effect of the fusion protein in an immuno-competent syngeneic mouse tumor model and in immuno-suppressed mice carrying subcutaneous human HER-2 positive tumors (Kwok C.S. et al, AACR Proceedings 42: 290-291, Abstract 1564, 2001). The investigation was later extended to a metastatic tumor model in SCID mice by injecting

intravenously into them human SKOV3 cells that over-express HER-2. Inhibitory effect of the FP on the growth of tumor nodules in the lungs was reported (Kwok C.S. et al, AACR Proceedings 43: 978, Abstract 4842, 2002). Three consecutive daily intravenous injections of 6 μg FP and 2 x 10^5 human peripheral blood mononulear cells (hPBMCs) into each of four SCID mice that had received 8 x 10^6 SKOV3 cells 3 days ago completely inhibited the development of lung metastasis four weeks later in all the animals. Treatment with 6 μg FP or 2 x 10^5 hPBMCs alone could only partially inhibit the growth of lung metastases. Vascular permeability changes in tumors and normal tissues that may be induced by FP, characterized by leakage of intravenously injected ^{125}I-labeled albumin into interstitial space of the tumors and tissues respectively at various times post intravenous injection of the FP, were also investigated in the syngeneic mouse tumor model and in nude mice carrying subcutaneous SKOV3 tumors. Specific increase in vascular permeability in the tumor compared with those in normal tissues was observed in the immuno-competent mice but not in the nude mice. Reasons for the difference in vascular permeability change caused by the FP in the two animal models are being explored. Such studies will help gain further insight into clinical applications of the FP.

Appendix 2

Kwok, C.S., Yip, T.C., Cheung, W.K., Leung, K.L., So, F.F., Ma, V.M. and Lau, W.H. "Recent advances of a novel vasoactive human interleukin-2/single chain antibody fusion protein for HER-2 positive tumors" *Proceedings of the 93rd American Association of Cancer Research*, San Francisco, LA, 6-10 April, 2002, p.978 (2002)

This study is a continuing effort to develop and characterize a novel vasoactive immuno-conjugate for treating HER-2 positive tumors refractory to conventional therapies. We had previously reported the construction of a fusion protein consisting of a recombinant human IL-2 and a recombinant humanized single-chain Fv (sFv) antibody which combined the V_H and V_L portions of a murine mAb (520C9) specific for human HER-2 (Li et al. "Preparation and characterization of a recombinant humanized single-chain Fv antibody/human interleukin-2 fusion protein directed against the HER-2/*neu* (c-erbB2) proto-oncogene product, p185". *Tumor Targeting*, Vol. 4, pp.105-114 (1999). Preliminary experiments to characterize the anti-tumor effect of the fusion protein in a syngeneic mouse tumor model and in immuno-suppressed mice carrying subcutaneous human HER-2/*neu* positive tumors were also reported (Kwok et al. "A novel vasoactive human interleukin-2/single chain antibody fusion protein for HER-

2/*neu* positive tumors". *Proceedings of the 92nd American Association of Cancer Research*, New Orleans, LA, 24-28 March, 2001, pp. 290-291 (2001). We recently extended our investigation by developing a metastatic tumor model in SCID mice by injecting intravenously into them with human SKOV3 cells that overexpressed HER-2/*neu*. Tumor nodules in the lungs and in more severe cases the liver developed at various times after the injection of the SKOV3 tumor cells. The latent period of tumor development depended on the number of SKOV3 cells injected. The growth inhibitory effect and the vasoactive property of the fusion protein on this metastatic tumor model will be reported. Specific vascular changes at the tumor site, characterized by leakage of intravenously injected ^{125}I-labeled albumin into interstitial space of the tumor and immuno-histological staining of endothelial cells by means of a specific anti-VE-cadherin antibody, will be presented. Such studies will gain further insight into clinical applications of the fusion protein.

Appendix 3

Yip, T.C., Kwok, C.S., So, F.F., Lau, W.H., Leung, K.L., Cheung, W.K., Ma, V.M. and Ngan, K.C. "An aminoglycoside antibiotic, Geneticin, can inhibit the growth of a HER-2 positive ovarian cancer in SCID mice model". *Proceedings of the 93rd American Association of Cancer Research*, San Francisco, LA, 6-10 April, 2002, p.923 (2002)

Tetracycline is a safe and inexpensive (less than US$1 per capsule) antibiotics that has been used for decades. Recent finding in prevent the spread of distant metatasis of breast and prostate cancers in mice probably through the inhibition of matrix metalloproteinase activity (Duivenvoorden, et al., Invasion Metatasis, Vol. 17(6), pp.312-322, 1997) has rekindled the interest in this antibiotic for cancer treatment. Tetracycline can inhibit bacterial protein synthesis by binding to 30S ribosomal RNA. Using an aminoglycoside antibiotics, Geneticin (G418), which has the same mechanism of action, we reported in this paper the in vivo growth inhibition effect of this antibiotic in a HER-2 positive ovarian cancer, SKOV-3 in SCID mice model. In the first series of experiments, saline or Geneticin at a concentration of 30, 125 and 500mg/ml were concurrently injected intramuscularly onto the trunk of the SCID mice together with $2x10^6$ SKOV3 tumor cells. The tumor was completely inhibited from growth by 125 and 500mg/ml

Geneticin at day 45 after injection. There was a 83% reduction of tumor mass (or a growth delay of ~32 days) at 30mg/ml when compared with saline control. In comparison, injection of Tetracycline only at a concentration of 500mg/ml but not at 30 or 125mg/ml resulted in significant tumor mass reduction. To further investigate the cytotoxic effect of Geneticin, SKOV-3 tumor was grown to an average size of $76mm^3$ (SD 42mm) before Geneticin was injected. Reduction of tumor mass of 30%, 42% and 67% in a concentration dependent manner were respectively found at 30, 125 and 500mg/ml when compared with the saline control. Further findings in the extent of apoptosis and the inhibition on distant spread of tumor in lung will be presented. This tumor growth inhibition effect by a commonly used antibiotic opens up the possible usage of a much cheaper adjunct for preventing distant spread of breast and prostate cancer in conjunction with conventional primary treatment modality.

Appendix 4

One-way ANOVA and Post Hoc Tests results for treatment experiment 1 of immunotherapy protocol in metastatic model

Oneway

Descriptives

% area covered by metastatic foci

	N	Mean	Std. Deviation	Std. Error	95% Confidence Interval for Mean		Minimum	Maximum
					Lower Bound	Upper Bound		
6 μg H520C9sFv-rhIL-2 + human PBM cells	4	.7250	.2986	.1493	.2498	1.2002	.40	1.10
6 μg H520C9sFv-rhIL-2	4	17.0750	4.0966	2.0483	10.5563	23.5937	13.00	22.30
Human PBM cells	4	17.7000	1.5642	.7821	15.2110	20.1890	16.00	19.70
Saline	4	27.8500	2.9983	1.4992	23.0790	32.6210	23.90	31.00
Total	16	15.8375	10.3140	2.5785	10.3416	21.3334	.40	31.00

ANOVA

% area covered by metastatic foci

	Sum of Squares	df	Mean Square	F	Sig.
Between Groups	1510.753	3	503.584	71.157	.000
Within Groups	84.925	12	7.077		
Total	1595.678	15			

Post Hoc Tests

Multiple Comparisons

Dependent Variable: % area covered by metastatic foci

Scheffe

(I) Group	(J) Group	Mean Difference (I-J)	Std. Error	Sig.	95% Confidence Interval	
					Lower Bound	Upper Bound
6 μg H520C9sFv-rhIL-2 + human PBM cells	6 μg H520C9sFv-rhIL-2	-16.3500*	1.8811	.000	-22.4370	-10.2630
	Human PBM cells	-16.9750*	1.8811	.000	-23.0620	-10.8880
	Saline	-27.1250*	1.8811	.000	-33.2120	-21.0380
6 μg H520C9sFv-rhIL-2	6 μg H520C9sFv-rhIL-2 + human PBM cells	16.3500*	1.8811	.000	10.2630	22.4370
	Human PBM cells	-.6250	1.8811	.990	-6.7120	5.4620
	Saline	-10.7750*	1.8811	.001	-16.8620	-4.6880
Human PBM cells	6 μg H520C9sFv-rhIL-2 + human PBM cells	16.9750*	1.8811	.000	10.8880	23.0620
	6 μg H520C9sFv-rhIL-2	.6250	1.8811	.990	-5.4620	6.7120
	Saline	-10.1500*	1.8811	.002	-16.2370	-4.0630
Saline	6 μg H520C9sFv-rhIL-2 + human PBM cells	27.1250*	1.8811	.000	21.0380	33.2120
	6 μg H520C9sFv-rhIL-2	10.7750*	1.8811	.001	4.6880	16.8620
	Human PBM cells	10.1500*	1.8811	.002	4.0630	16.2370

*. The mean difference is significant at the .05 level.

Appendix 5

One-way ANOVA and Post Hoc Tests results for treatment experiment 2 of immunotherapy protocol in metastatic model

Oneway

Descriptives

% area covered by metastatic tumor foci

	N	Mean	Std. Deviation	Std. Error	95% Confidence Interval for Mean		Minimum	Maximum
					Lower Bound	Upper Bound		
6 μg H520C9sFv-rhIL-2 + human PBM cells	4	.2250	.1893	9.465E-02	-7.62E-02	.5262	.10	.50
3 μg H520C9sFv-rhIL-2 + human PBM cells	4	24.7000	5.6892	2.8446	15.6473	33.7527	16.60	29.80
Saline	4	29.1750	7.6921	3.8461	16.9351	41.4149	20.70	36.60
Total	12	18.0333	14.1985	4.0988	9.0120	27.0547	.10	36.60

ANOVA

% area covered by metastatic tumor foci

	Sum of Squares	df	Mean Square	F	Sig.
Between Groups	1942.872	2	971.436	31.825	.000
Within Groups	274.715	9	30.524		
Total	2217.587	11			

Post Hoc Tests

Multiple Comparisons

Dependent Variable: % area covered by metastatic tumor foci

Scheffe

(I) group	(J) group	Mean Difference (I-J)	Std. Error	Sig.	95% Confidence Interval	
					Lower Bound	Upper Bound
6 μg H520C9sFv-rhIL-2 + human PBM cells	3 μg H520C9sFv-rhIL-2 + human PBM cells	-24.4750*	3.9067	.001	-35.8735	-13.0765
	Saline	-28.9500*	3.9067	.000	-40.3485	-17.5515
3 μg H520C9sFv-rhIL-2 + human PBM cells	6 μg H520C9sFv-rhIL-2 + human PBM cells	24.4750*	3.9067	.001	13.0765	35.8735
	Saline	-4.4750	3.9067	.542	-15.8735	6.9235
Saline	6 μg H520C9sFv-rhIL-2 + human PBM cells	28.9500*	3.9067	.000	17.5515	40.3485
	3 μg H520C9sFv-rhIL-2 + human PBM cells	4.4750	3.9067	.542	-6.9235	15.8735

*. The mean difference is significant at the .05 level.